NTNU
Det skapende universitet

Undersøkelse av småturbin

Cecilie Kvangarsnes

NTNU

Norges teknisk-
naturvitenskapelige universitet

Institutt for energi- og prosessteknikk

EPT-M-2012-56

MASTEROPPGAVE

for

Stud.techn. Cecilie Kvangarsnes

Våren 2012

Undersøkelse av småturbin

Inevestigation of a small hydro turbine

Bakgrunn og målsetting

En småturbin av Kaplan-typen er installert i Vannkraftlaboratoriet. Den er produsert i Afghanistan og blir brukt for å produsere elektrisk kraft i landsbyer. Av produksjonsmessige hensyn er designen sterkt forenklet. Turbinen har ikke regulerbart ledeapparat, men skovlvinklene til løpehjulet kan endres ved at skovlene settes i forskjellige posisjoner.

Det er i høstsemesteret 2011 gjennomført en prosjektoppgave og en Masteroppgave med turbinen som objekt. I prosjektoppgaven ble virkningsgrader målt, men man oppnådde ikke å dekke hele område. Det gjenstår også å måle virkningsgrader på to løpehjulsvinkler. I masteroppgaven ble det gjort en 2D simulering med CFD med formål å foreslå forbedring av innløpet til turbinhjulet.

Målet med denne masteroppgaven er å måle virkningsgrad ved høyere last, samt å lage en 3D CFD modell for bedre analyse av innløpet.

Kandidaten vil samarbeide med PhD student Kaunda fra Dar es Salam University under den eksperimentelle delen

Oppgaven bearbeides ut fra følgende punkter

1. Sette seg inn i tidligere arbeid med turbinen

2. Foreslå systemendringer for å kunne observere kavitasjon

3. Måle virkningsgrader og lage Hill-diagram for to forskjellige løpehjulsvinkler

4. Lage 3D CFD modell av turbinens innløp og foreslå endringer av kaskadebend og ledeskovler

Senest 14 dager etter utlevering av oppgaven skal kandidaten levere/sende instituttet en detaljert fremdrift- og eventuelt forsøksplan for oppgaven til evaluering og eventuelt diskusjon med faglig ansvarlig/veiledere. Detaljer ved eventuell utførelse av dataprogrammer skal avtales nærmere i samråd med faglig ansvarlig.

Besvarelsen redigeres mest mulig som en forskningsrapport med et sammendrag både på norsk og engelsk, konklusjon, litteraturliste, innholdsfortegnelse etc. Ved utarbeidelsen av teksten skal kandidaten legge vekt på å gjøre teksten oversiktlig og velskrevet. Med henblikk på lesning av besvarelsen er det viktig at de nødvendige henvisninger for korresponderende steder i tekst, tabeller og figurer anføres på begge steder. Ved bedømmelsen legges det stor vekt på at resultatene er grundig bearbeidet, at de oppstilles tabellarisk og/eller grafisk på en oversiktlig måte, og at de er diskutert utførlig.

Alle benyttede kilder, også muntlige opplysninger, skal oppgis på fullstendig måte. For tidsskrifter og bøker oppgis forfatter, tittel, årgang, sidetall og eventuelt figurnummer.

Det forutsettes at kandidaten tar initiativ til og holder nødvendig kontakt med faglærer og veileder(e). Kandidaten skal rette seg etter de reglementer og retningslinjer som gjelder ved alle (andre) fagmiljøer som kandidaten har kontakt med gjennom sin utførelse av oppgaven, samt etter eventuelle pålegg fra Institutt for energi- og prosessteknikk.

Risikovurdering av kandidatens arbeid skal gjennomføres i henhold til instituttets prosedyrer. Risikovurderingen skal dokumenteres og inngå som del av besvarelsen. Hendelser relatert til kandidatens arbeid med uheldig innvirkning på helse, miljø eller sikkerhet, skal dokumenteres og inngå som en del av besvarelsen.

I henhold til "Utfyllende regler til studieforskriften for teknologistudiet/sivilingeniørstudiet" ved NTNU § 20, forbeholder instituttet seg retten til å benytte alle resultater og data til undervisnings- og forskningsformål, samt til fremtidige publikasjoner.

Besvarelsen leveres digitalt i DAIM. Et faglig sammendrag med oppgavens tittel, kandidatens navn, veileders navn, årstall, instituttnavn, og NTNUs logo og navn, leveres til instituttet som en separat pdf-fil. Etter avtale leveres besvarelse og evt. annet materiale til veileder i digitalt format.

NTNU, Institutt for energi- og prosessteknikk, 17. januar 2012

Olav Bolland
Instituttleder

Torbjørn K. Nielsen
Faglig ansvarlig/veileder

Preface

This thesis has been a combination of laboratory work and CFD simulations, giving me a good insight in both practical and theoretical issues related to turbine design and optimisation. I am thankful for this opportunity to get hands on experience and to improve my understanding of a hydrological system.

I want to thank Anders Austegård for giving me the opportunity to work on this turbine, and for the discussion in the beginning of my thesis. I also want to thank my supervisor Professor Torbjørn Nielsen for always keeping an open door to his office. Big thanks also goes to Peter Joachim Gogstad for always being available for questions and help when needed.

Bård Brandåstrø, Joar Hilstad, Halvor Haukvik and Trygve Opland deserves big thanks for all the help in the laboratory. Without them the laboratory work would not have been possible to carry out. Trygve deserves extra thanks for all his hours spent struggling with the turbine.

Finally, I want to give huge thanks to Remi Andrè Stople for sharing all his previous experience with me and discussing the results. Thanks also to Bjørn Winther Solemslie and Martin Aasved Holst for assistance with computational programs, and the other students at the Waterpower Laboratory for making a good atmosphere and working environment.

NTNU Trondheim, June 24, 2012
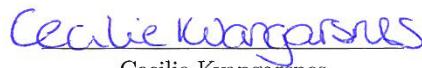
Cecilie Kvangarsnes

Abstract

In this thesis a Kaplan type turbine produced in Afghanistan has been investigated. A full efficiency analysis is done in the laboratory, on two out of four runner vane settings. Just before the turbine inlet, there is a 90 degree bend, that has been simulated in Ansys Fluent. Improvements of the bend have been suggested.

The turbine is manufactured by Remote HydroLight for use in Afghanistan. The aim of the turbine is to make the design uncomplicated enough for the inhabitants to produce and maintain the plant on their own. This means the turbine has to be modified compared to a traditional Kaplan turbine. In other words, a non complex structure is more important than a high efficiency.

Given the simplified condition of the turbine, the best efficiency point found was very high; 85.32 % for runner vane setting 1, and 87.75 % for setting 2, with an uncertainty of 0.5 %. Reduced parameters were used. Increasing the pressure head, the efficiency increased slightly. It is believed that this is caused by decreased friction loss with increased Reynolds number. For setting 2, the opposite effect was seen; the efficiency decreased slightly with higher pressure head for high volume flows. This can be caused by increased loss in the turbine because of a higher disturbance of the flow after the bend, for high volume flows.

The runner vanes can be changed to four different positions, while the guide vanes are not adjustable. The positions are marked with indents on the runner vanes, and finding the exact same position once moved is difficult. Measurements done on the same runner vane positions will therefore vary.

The bend has two flow controllers and the effect of this has been simulated. The simulations show that the lower flow controller has a large positive effect, distributing the flow better than with no flow controllers. The upper flow controller does not show much additional effect on the flow, and can therefore be removed. Moving the lower flow controller to the right, has an additional positive effect on the flow, accelerating the flow in the inner part of the bend. The simulations have been compared to Pitot measurements done in the laboratory, showing the same tendencies in the flow.

iv

Sammendrag

I denne oppgaven har en Kaplan turbin produsert i Afghanistan blitt undersøkt. En fullstendig virkningsgradanalyse er gjort i laboratoriet, på to av fire løpehjulsvinkler. Like før innløpet til turbinen er det et 90 grader bend, som har blitt simulert i Ansys Fluent. Forbedringer av bendet er foreslått.

Turbinen er laget av Remote HydroLight for bruk i Afghanistan. Målet med turbinen er at oppbygningen er enkel nok til at innbyggerne kan produsere og vedlikeholde turbinen på egenhånd. Det betyr at turbinen må være modifisert i forhold til en tradisjonell Kaplan turbin. Sagt med andre ord, er et enkelt design viktigere enn en høy virkningsgrad.

Forenklingene av turbindesignet tatt i betraktning, er beste virkningsgrad høy; 85.32 % for løpehjulsposisjon 1, og 87.75 % for posisjon 2, med en usikkerhet på 0.5 %. Reduserte parametere er brukt. Dersom fallhøyden økes, ser man en liten økning i virkningsgraden. Dette kan skyldes lavere friksjonstap ved høyere Reynolds tall. For posisjon 2 ser man den motsatte effekten; virkningsgraden minker litt med høyere fallhøyde, for høy volumstrøm. Dette kan være fordi høyere volumstrøm gir høyere tap i bendet, fordi strømningsprofilen blir mer ujevn.

Løpehjulskovlene har fire ulike posisjoner, mens ledeskovlene ikke kan justeres. Posisjonene er markert med små hakk på bladene, og å finne eksakt samme posisjon når skovlene har blitt flyttet på er vanskelig. Målinger gjort på samme skovlåpning gir derfor varierende resultat.

Bendet har to strømningsrettere og effekten av disse har blitt simulert. Simuleringene viser at den nedre strømningsretteren har en stor positiv effekt på strømningen i forhold til å ikke ha strømningsrettere. Den øvre strømningsretteren viser liten eller ingen effekt på strømningen og kan derfor bli fjernet. Dersom den nedre strømningsretteren flyttes mot høyre, er den positive effekten på strømningen enda større, ved at den akselererer strømningen i den indre delen av bendet. Simuleringer har blitt sammenlignet med Pitot-målinger gjort i laboratoriet, og de viser de samme tendensene i strømningen.

Contents

List of Figures

List of Tables

Nomenclature

Symbol	Description	Unit
A	cross section area	[m^2]
D	diameter	[m]
D$_t$	turbine diameter	[m]
E$_{pot}$	potential energy	[J]
f	Darcy friction factor	[-]
g	gravity constant	[m/s^2]
h	head	[m]
H$_e$	effective pressure head	[m]
m	mass	[kg]
n	rotaional speed	[rpm]
n$_{ed}$	reduced rotational speed	[-]
P$_{pot}$	potential power	[W]
P$_m$	mechanical power	[W]
P$_h$	hydraulic power	[W]
p	pressure	[Pa]
p$_{atm}$	atmospheric pressure	[Pa]
Q	volume flow	[m^3/s]
Q$_{ed}$	reduced volume flow	[-]
T	torque	[Nm]
v	velocity	[m/s]
V	specific volume	[m^3/kg]
z	distance	[m]
η	efficiency	[%]
ρ	density	[kg/m^3]
μ	viscosity	[kg/ms]
θ	water temperature	[°C]
ω	rotational speed	[s^{-1}]

Chapter 1

Introduction and background

1.1 Energy situation in Afghanistan today

According to the World Bank, only 15.6 % of the population in Afghanistan had access to electricity in 2009 (World Bank, 2012). The electricity is mostly imported (72.8 %), about a fourth from hydro power (26 %) and a small share from thermal sources (1.3 %) (AEIC, 2012). Because of the lack of transmission lines, most electricity is available only in the areas with the highest population density, leaving the villages with zero or little electricity access. The share of population that is connected to the electricity grid in Afghanistan is showed in figure 1.1.
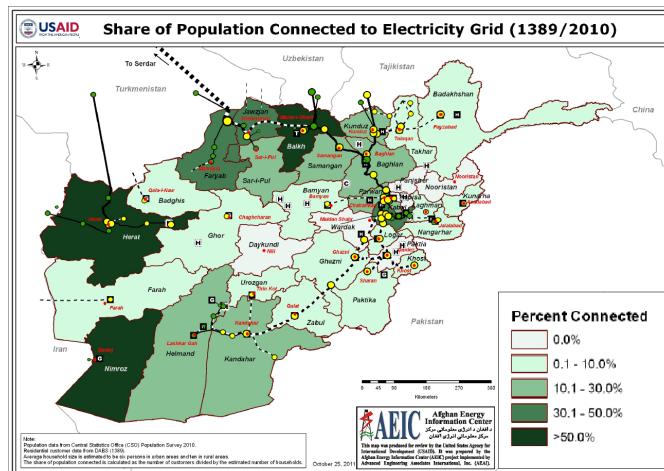
Figure 1.1: Share of population connected to the electricity grid

The lack of electricity access makes the use of kerosone (paraffin lamp) a common source of lighting. For cooking and heating, wood is being used. This is highly time consuming, involves health hazards and chopping down the forest is bad for the environment.

Making of micro hydropower plants which are owned and payed for by the community is now a growing alternative in Afghani villages. The plants give employment opportunities for the inhabitants and electricity to the village. It gives light and energy for cooking and heating as well as for processing of agricultural products. Other small scale electricity sources are wind, solar, geothermal energy and biogas. These are all renewable sources of energy with zero or little emissions.

Afghanistan is one of the poorest and least developed countries in the world and the country is highly dependent on foreign aid.

1.2   Remote HydroLight

Remote HydroLight works on manufacturing and installing micro-hydro power plants in Afghanistan, as well as training the inhabitants to use and maintain the plants (Remote HydroLight, 2012). The aim is to manufacture plants that are easy to build and maintain in order to be self helped and able to fix problems that occur during production. The power production is small enough for the village to consume the electricity themselves without the need for big transmission lines.

Anders Austegård works for Remote HydroLight and lives in Afghanistan most of the year. He has designed a Kaplan type turbine that is installed in several Afghani villages. One turbine has been installed at the water power laboratory at NTNU, in order to do efficiency tests and suggest improvements.

The turbine runner has four runner vane settings, where setting 1 gives the lowest volume flow and setting 4 the largest. Remote Hydrolight has requested that the turbine is tested with a pressure head between 2-8 meter and rotational speed between 500-1100 rpm on all four runner vane settings. It is desirable to make a complete Hill diagram and find the best operation point, in order to fully understand how the turbine operates.

The flow gets disturbed by a 90 degree bend in front of the turbine inlet. It is desirable to improve the conditions in the bend in order to get a more uniform flow into the turbine. These improvements should not make the turbine more complex or more expensive to produce.

1.3   Scope of work

The aim of this thesis is to measure the efficiency of a Kaplan type turbine produced in Afghanistan, and to investigate the velocity profile in a 90 degree bend just before

the turbine inlet. The thesis is a combination of measurements in the laboratory and CFD simulations. A PhD student from Dar es Salam University was supposed to cooperate on the experimental part of the thesis, but could not come because of problems with the paper work.

1.3.1 Limitations done in this thesis

Anders Austegård required test results with a pressure head of 2 to 8 meter and a rotational speed on the turbine from 500 to 1100 rpm to be done on all 4 runner vane settings. The turbine is made too big for the turbine housing in order to "self-grind" and make the gap between the turbine and the turbine housing as small as possible. Stople and Fjærvold (Stople, 2011 and Fjærvold, 2011) spent a lot of time grinding setting 1 and 2. Trying to move the runner vanes to setting 3, the turbine got stuck in the housing. Austegård recommended to move the turbine slightly up in the housing. After several discussions with Professor Torbjørn Nielsen, Bård Brandåstrø and the mechanics in the laboratory it was decided not to do measurements on settings 3 and 4 because of the additional work and the limitation in time. Complete efficiency tests will be done on runner vane setting 1 and 2.

Cavitation problems is agreed with supervisor Torbjørn Nielsen not to be looked at.

Chapter 2

Theory

2.1 Hydro power plant

A hydro power plant makes use of the potential energy stored in elevated water to produce electricity. Hydro power is a renewable source of energy and has zero emissions. A typical hydro power structure is shown in figure 2.1 (Dahlhaug, 2012).
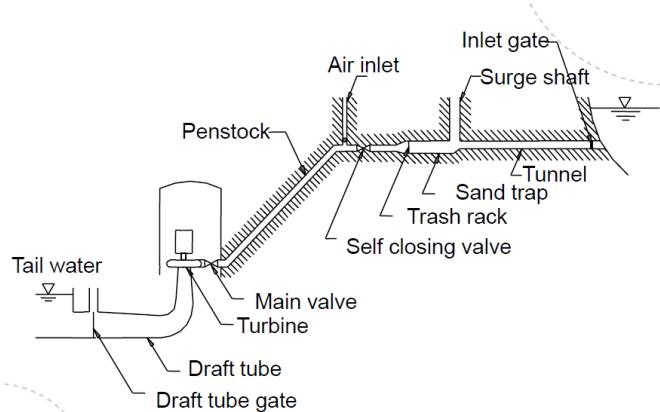
Figure 2.1: Hydro power plant

The potential energy is given by equation (2.1).

$$E_{pot} = mgh \quad [J] \tag{2.1}$$

This gives the total available power shown in equation (2.2).

$$P_{pot} = \rho Q g h \quad [W] \tag{2.2}$$

2.1.1   Hydraulic efficiency

The hydraulic efficiency is defined as the output mechanical power from the turbine, relative to the available hydraulic power. The output power is given as the shaft torque times the rotational speed as shown in equation (2.3). The available hydraulic power is given by equation (2.4), where H_e is the effective pressure head. H_e is given by Bernoulli's equation (2.5) (White, 2008, p.188).

$$P_m = T\omega \quad [W] \quad \text{where} \quad \omega = \frac{2\pi n}{60} \quad [s^{-1}] \tag{2.3}$$

$$P_h = \rho \cdot Q \cdot g \cdot H_e \quad [W] \tag{2.4}$$

$$H_e = \frac{p_1 - p_2}{\rho g} + \frac{v_1^2 - v_2^2}{2g} + z_1 - z_2 \quad [m] \tag{2.5}$$

In equation 2.5, the indexes 1 and 2 represents the system inlet and outlet, respectively. This is shown in figure 2.8.

The efficiency is found by dividing the output mechanical power with the available hydraulic power, as seen in equation (2.6).

$$\text{Total efficiency}: \eta = \frac{P_m}{P_h} = \frac{T \cdot 2\pi \cdot n}{60 \cdot \rho \cdot Q \cdot g \cdot H_e} \tag{2.6}$$

2.1.2   Reduced parameters

In order to make general statements, reduced parameters are used. Reduced parameters are dimensionless, and the reduced parameters Q_{ed} and n_{ed} are shown in equation (2.7) and (2.8).

$$Q_{ed} = \frac{Q}{D^2 \sqrt{g \cdot H_e}} \tag{2.7}$$

$$n_{ed} = \frac{n \cdot D}{\sqrt{g \cdot H_e}} \tag{2.8}$$

2.1.3   Velocity measurements

There are different ways to measure flow velocities, Pitot measurements being one of them. Pitot measurements are described in Fluid Mechanics (White, 2008, p 405). Pitot measurements are based on Bernoulli's equation (2.5), as shown in equation (2.9), where p_s is static pressure and p_0 is the stagnation pressure. At the stagnation point the velocity is zero.

$$p_s + \frac{\rho v^2}{2} + \rho g z_s = p_0 + \frac{\rho 0^2}{2} + \rho g z_0 \tag{2.9}$$

If the distance z_0 - z_s is neglectable we get equation (2.10).

$$v = \sqrt{2\frac{p_0 - p_s}{\rho}} \tag{2.10}$$

Equation (2.10) can be re-written as equation (2.11).

$$v = \sqrt{2g\Delta h} \quad \text{where} \quad p_0 - p_s = \rho g \Delta h \tag{2.11}$$

When doing Pitot measurements, the pitot tube itself will slightly disturb the velocity flow.

2.1.4   Turbulence and Moody diagram

Turbulence is three-dimensional, unsteady, random motion in fluids at moderate to high Reynolds numbers. The Reynolds number is defined in equation (2.12).

$$Re = \frac{\rho \cdot v \cdot D}{\mu} \tag{2.12}$$

In a Moody diagram shown in figure 2.2, the friction factor, relative roughness of the walls and the Reynolds number is plotted. The friction factor, f, is high for low Reynolds numbers, and low for high Reynolds number.
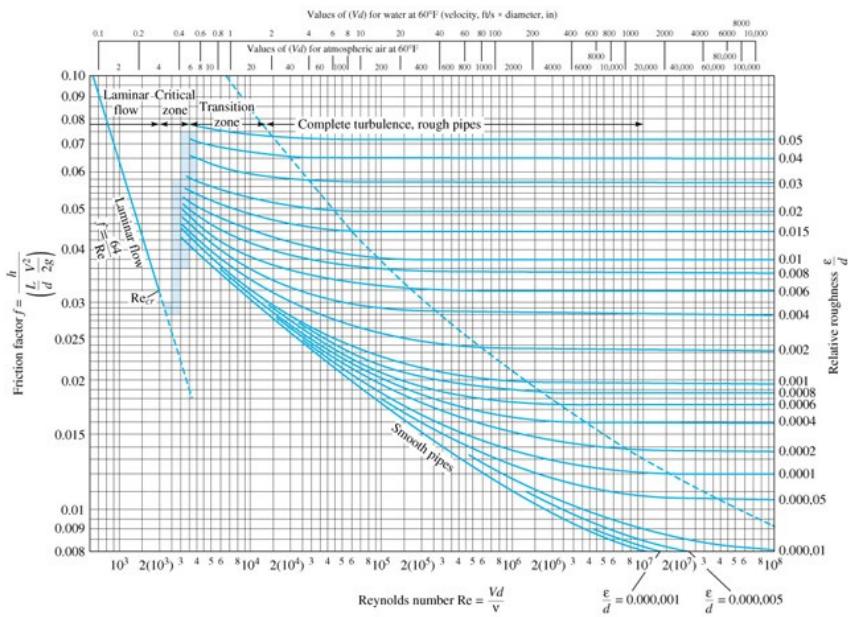
Figure 2.2: Moody diagram

2.1.5 Cavitation

When fluid velocity increases, the pressure will decrease if the temperature is constant (pV=const). If the pressure gets below the vapour pressure, bubbles will form. These bubbles will collapse when they reach an area with higher pressure, as shown in figure 2.3 (Dahlhaug, 2012). This happens in fractions of a second.
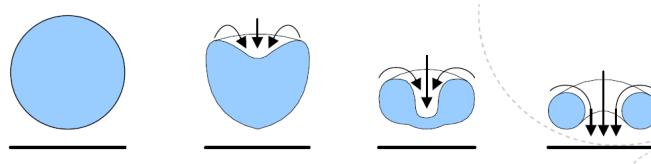
Figure 2.3: A collapsing bubble

When the bubble collapses a jet stream will be created as shown in figure 2.3. The jet stream will hit the surface with large impulse. The local pressure can cause great damage to the surface, formed as "craters". This will create a rougher surface and decrease the efficiency.

2.2 Kaplan turbine

The Kaplan turbine was developed by Austrian Victor Kaplan around 1913.

The Kaplan turbine is a reaction turbine and is typically used for low head (5m - 70m) and high flow rates (Brekke, 2000). It is mostly used in plants without magazines. The turbine has a spiral casing like the Francis turbine, which gives a constant velocity into the turbine runner. The runner vanes can be regarded as a further development from the propeller turbine, but with adjustable runner vanes. A Kaplan turbine is shown in figure 2.4.

Like the Francis turbine, the Kaplan also has a draft tube to regain pressure after the runner. It is recommended to dive the turbine in order to prevent cavitation at the runner outlet.
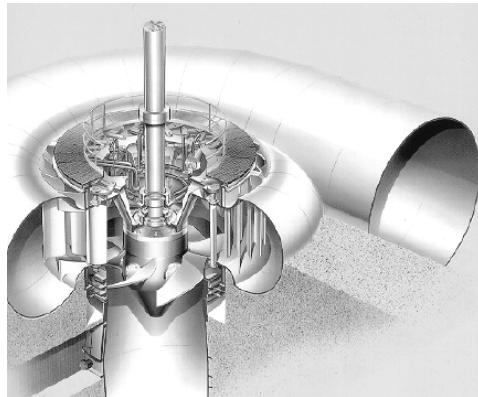
Figure 2.4: Kaplan turbine

2.2.1 Efficiency and Hill diagram

The Kaplan turbine has adjustable guide vanes and runner vanes like a Francis turbine. This gives a flat efficiency curve as shown in figure 2.5, when the relationship between the guide vanes and runner vanes are optimal (Brekke, 2003, p.109). This means that it can operate over a large range of flow rates, keeping a high efficiency.
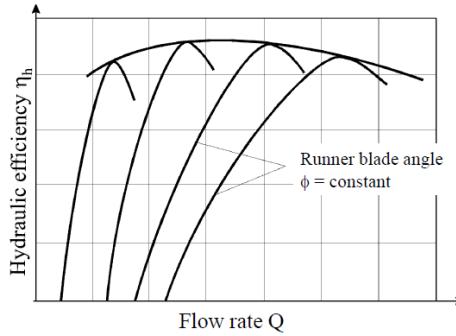
Figure 2.5: Efficiency curve for a Kaplan turbine with runner vane angle ϕ

In figure 2.6 the efficiencies of a Kaplan turbine are combined in a Hill diagram.
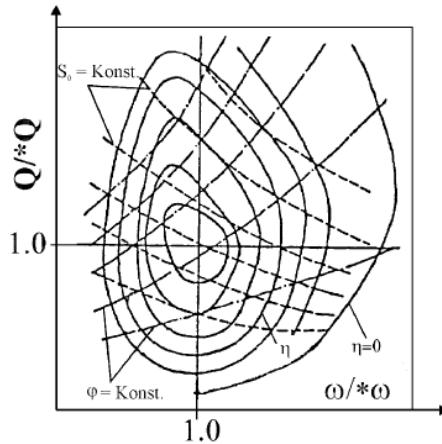
Figure 2.6: Hill diagram for a Kaplan turbine

2.3   The Afghanistan turbine

The Afghanistan turbine is designed by Anders Austegård. The fact that it is easy to manufacture is more important than getting a high efficiency. This turbine therefore is a simplified version of the Kaplan turbine. It does not have a spiral casing and the guide vanes are not adjustable. The runner vanes can be adjusted by hand to four different positions, named setting 1-4, which are being used depending on the pressure head and volume flow available.

The turbine is a vertical turbine with the shaft going from the turbine, through the inlet pipe and bend, to the generator placed on top of it.

The Afghanistan turbine has been drawn in Inventor by Austegård and is shown in figure 2.7.
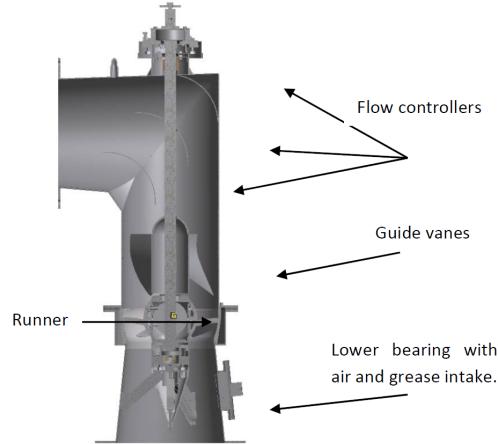
Figure 2.7: The Afghanistan Turbine

In this thesis the whole turbine system is considered, not only the turbine runner itself. The hydraulic efficiency is measured from inlet to outlet as shown in figure 2.8.
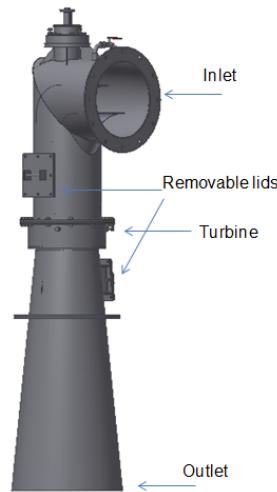
Figure 2.8: Definition of inlet and outlet

The main dimensions of the turbine is given in table 2.1

Table 2.1: Main dimensions of the turbine

D_t	Runner diameter	0.356 m
D_1	Inlet diameter	0.400 m
D_2	Outlet diameter	0.596 m
z	Distance between inlet and outlet	2.148 m

The different runner vane settings can be seen in figure 2.9. The runner vanes are adjusted step-wise by hand, with access from two lids as shown in figure 2.8. Once moving the runner vane, it is difficult to place it in the exact same position, and it takes a lot of patience because of the placing inside a tube with access only from above and below.

Figure 2.9: Runner vane with four settings - 90 degree bend before turbine - The generator is placed on top of the turbine

Figure 2.9 also shows the 90 degree bend before the turbine. There are reasons to believe that this bend creates non uniform streamlines into the turbine. In order to make the flow more uniform, a cascade of flow controllers are placed in the bend. This is shown in figure 2.7.

The generator is placed on top of the turbine as shown in figure 2.9. It has a maximum rotational speed of 1500 rpm and a maximum torque of 324.7 Nm. Additional information about the generator is given in appendix E.

Chapter 3

Former work

Remi Andrè Stople and Lars Fjærvold did their project and master thesis, respectively, on the Afghanistan turbine during autumn 2011 (Stople, 2011 and Fjærvold, 2011). They installed the turbine in the laboratory and did measurements on efficiency and clearance water, and made suggestions on how to observe cavitation. It was not possible to do measurements with large flow rates and low pressure heads, due to under-dimensioning of the rig and the measurements done had high uncertainties. Measurements were done for setting 1 and 2, but complete tests could not be done. It was therefore necessary to rebuild the rig.

Efficiencies were found for pressure heads between 2.5 and 6 meters. The best efficiency at setting 1 and 2 is shown in table 3.1 (Stople, 2011). This is not the best efficiency point, because complete measurements are not done.

Table 3.1: Best efficiency, Stople and Fjærvold

	Efficiency	Effective head	Rotational speed
Setting 1	$76.4 \pm 1.58\,\%$	2.25 m	552 rpm
Setting 2	$83.9 \pm 1.58\,\%$	2.75 m	600 rpm

It was concluded that the efficiency is reasonably high considered the design, but the measurements has high uncertainties. The tests also showed that the turbine performance is good for a wide range of pressure heads.

Fjærvold also did a 2D CFD analysis of the inlet bend with the conclusions that the bend should be rounded and that the guide vanes should cover the whole diameter of the bend in order to get a more even velocity distribution (Fjærvold, 2011). He also concluded that the design of the turbine itself was satisfying.

The turbine originally had two steal covers that could be opened in order to adjust the runner vanes; one above the runner and one below. The one below was replaced with a Plexi glass cover in order to observe cavitation with a high speed camera, but mist made it impossible to observe.

There were some problems with heating of the upper bearing, especially during tests at high volume flow combined with high rotational speed.

The clearance water test showed that the clearance water is dependent on the pressure head alone. Large pressure head gives more clearance water than smaller pressure heads. It was concluded that the clearance water is low compared to the volume flow, and can be neglected.

Chapter 4

Experimental setup and methode

4.1 Rig set up

An overview of the rig set up in the laboratory is given in figure 4.1. Water is pumped from the reservoir into a pressure tank. From the pressure tank the water runs through the turbine back into the reservoir.
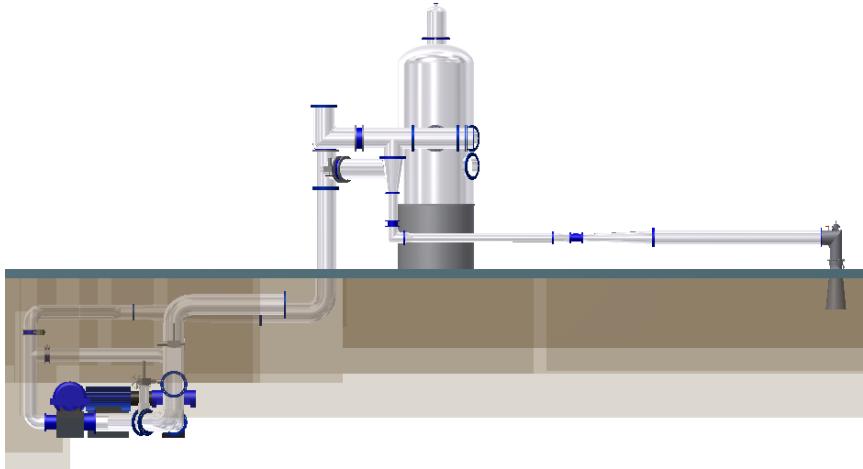
Figure 4.1: Set up of the rig in the laboratory

To calculate the efficiency, different instruments are used to measure torque on the

shaft, volume flow, pressure head and the rotational speed of the turbine. The pumps are controlled with a remote computer to keep the pressure head constant.

The start up procedure of the system is given in appendix A

4.2   Instrumentation and calibration

IEC 60193 (IEC, 1999) is an international standard given by the International Electrotechnical Commission on *Model acceptance tests on Hydraulic turbines, storage pumps and pump-turbines.* All the tests in the laboratory are based on the *Norwegian electrotechnical publication* of this standard.

The instruments send voltage signals to a computer via a logging card. The logging card registers the voltage signals continuously and feeds them into a LabView program. LabView converts the signals to the correct values, using calibrated values.

Calibration of the instruments are done with both increasing and decreasing load in order to get better results. Calibration is done once before starting the tests and once after all tests are finished. The calibration program is made by Bjørn Winther Solemslie.

4.2.1   Torque transducer

The torque transducer is placed on the shaft between the turbine and the generator. The upward shaft is connected to the generator, and while calibrating the torque transducer an arm keeps it from moving. A moment arm is connected to the downward shaft. From the arm, a wire goes via a wheel to a dish where calibrated weights of 2 and 5 kg are placed. The calibration report of the weights is attached in appendix B.1. Equation (4.1) is used to calculate the torque.

$$\text{Torque} = \text{ moment arm } \cdot \text{ mass } \cdot \text{ gravitation} \qquad (4.1)$$

The length of the moment arm and mass of the dish and wire are shown in table 4.1.

Table 4.1: Length of arm, and mass of the dish and wire

Dish	4.7465 kg
Wire	0.04175 kg
Total mass, dish and wire	**4.78825 kg**
Radius shaft	0.0525 m
Additional arm	0.469 m
Total arm	**0.5215 m**

Calibration of the torque is shown in figure 4.2.

Figure 4.2: Calibrating the torque transducer

The transducer has a range of $\pm$ 1000 Nm and gives voltage signal of $\pm$ 10 V. Because the transducer is placed upside down, positive torque gives negative readings. The transducer is only calibrated to 400 Nm, because this will cover the desired measurements.

Because the efficiency is considered between the inlet and outlet of the whole turbine system, not just the turbine runner, the friction torque is not considered.

The calibrated torque curve is given in figure 4.3 and the formula is given in equation (4.2).
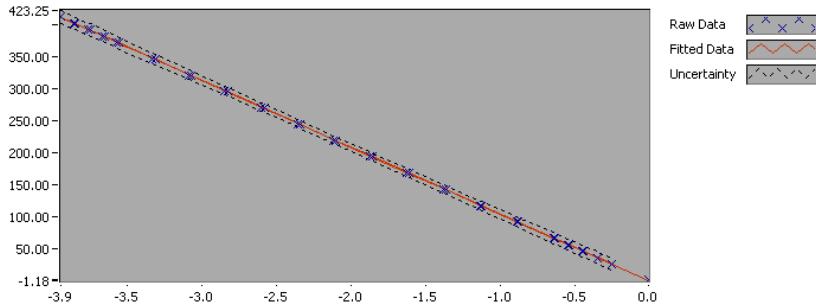
Figure 4.3: Calibrated curve, torque

$$y = 105.10908427x + 2.08223707 \tag{4.2}$$

The calibration report for the torque transducer is attached in appendix B.1.

4.2.2   Pressure transducer

The inlet pressure is measured just before the inlet of the turbine system. The pressure transducer is fed by four taps equally distributed around the pipe as shown in figure 4.4. The outlet pressure is calculated.

The pressure transducer, a Druck PTX1400, is calibrated by pumping air with known pressure into the calibrator, a Digital Pressure Indicator DPI601, and register the voltage signal that corresponds to this given pressure.

Figure 4.4: Calibrating the pressure transducer

The pressure is measured in millibars, $1\,\text{bar} = 10^5\,\text{Pa}$, up to 2 bars. The atmospheric pressure (zero point) varies from day to day, and has to be adjusted for while running tests.

The calibrated pressure curve is given in figure 4.5 and the formula is given in equation (4.3).
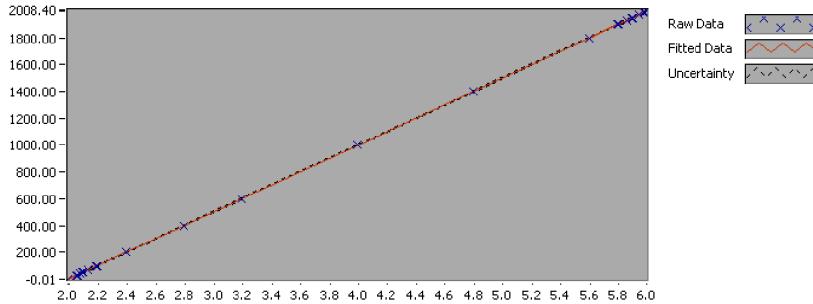
Figure 4.5: Calibrated curve, inlet pressure

$$y = 499.83841396x - 995.10178147 \tag{4.3}$$

The calibration report for the pressure transducer is attached in appendix B.2.

4.2.3 Trip meter

A reflex tape is placed on the shaft. When calibrating the trip meter, a digital trip meter, Digital Tachometer, HT-431, is held towards the reflex tape and registers how frequent the tape passes the trip meter. The rotational speed in rotations per minute (rpm) can be read in the display and calibrated towards the given voltage signal. This is shown in figure 4.6.

Figure 4.6: Calibrating the trip meter

The calibrated pressure curve is given in figure 4.7 and the formula is given in equation (4.4).
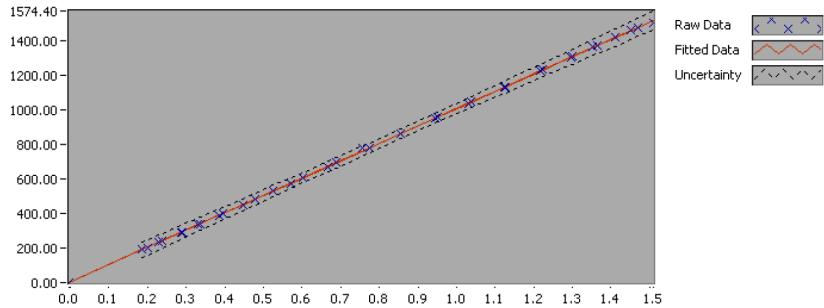
Figure 4.7: Calibrated curve, trip meter

$$y = 1003.90144x + 4.18733037 \tag{4.4}$$

The calibration report for the trip meter is attached in appendix B.3.

4.2.4   Volume flow meter

The volume flow has not been calibrated because it was calibrated recently by Stople and Fjærvold. In order to calibrate the flow meter again, the pipes would have to be rebuilt to lead the water into the calibration tank. The calibration formula is shown in equation (4.5) (Stople, 2011, p.31).

$$y = 81.49352283x - 162.87533823 \tag{4.5}$$

4.2.5   Atmospheric pressure and water temperature

The atmospheric pressure and water temperature are measured continuously in the laboratory. The water temperature is measured by a digital temperature sensor in the sump near the weighting tank. The calibration certificates are given in appendix B.5.

4.3   Logging of results in LabView

A logging program is made in LabView by Remi Andre Stople, with a logging frequency of 1000 per second. The raw data is stored in a text file for post treatment. The constant of gravity is shown in equation (4.6). It was measured at NTNU in 2004, and the calibration report is attached in appendix B.4.

$$g = 9.82146514 m/s^2 \tag{4.6}$$

The density of water and the outlet pressure is calculated in LabView.

Density of water

The equation for calculating water density is shown in equation (4.7) (IEC, 1999, p.171).

$$\frac{1}{\rho} = V_0[(1 - A \cdot p) + 8 \cdot 10^{-6} \cdot (\theta - B + C \cdot p)^2 - 6 \cdot 10^{-8} \cdot (\theta - B + C \cdot p)^3]$$

where $\tag{4.7}$

$V_0 = 1 \cdot 10^{-3} m^3 \cdot \text{kg}^{-1}$

$A = 4.6699 \cdot 10^{-10}$

$B = 4.0$

$C = 2.1318913 \cdot 10^{-7}$

$\theta = \text{temperature in } °C$

$p = p_{abs} \text{ in } Pa$

Absolute pressure, p_{abs}, is the sum of atmospheric pressure and gauge pressure. Atmospheric pressure is fed into LabView before starting the tests and the gauge pressure is measured continuously. The water temperature increases slightly while running tests, and is adjusted a few times during running.

Outlet pressure

The height difference between the outlet and the tail water equals the static pressure at the outlet, $p_{s,2}$. To get the outlet pressure p_2, the hydraulic pressure has to be subtracted. The outlet pressure is given by equation (4.8). It is found that while running tests, the tail water sinks with approximately 15 cm, because of the water in the piping system.

$$p_2 = p_{s,2} - \frac{v_2^2}{2g} \quad [m] \tag{4.8}$$

4.4 Test Matrix

Two series of measurements are done in the laboratory on runner vane setting 1 and 2, with a constant pressure head of 3.5 and 5 meters, respectively, and rotational

speed of 400 to 1400 rpm. This corresponds to the requested measurements from Austegård, using reduced parameters. The test matrix is shown in table 4.2.

Table 4.2: Test matrix

Rpm	Setting 1		Setting 2	
	3.5 m	5 m	3.5 m	5 m
400	x	x	x	x
450	x	x	x	x
500	x	x	x	x
550				
600	x	x	x	x
650				
700	x	x	x	x
750	x	x	x	x
800	x	x	x	x
850	x	x	x	x
900	x	x	x	x
950	x	x	x	x
1000	x	x	x	x
1050	x	x	x	x
1100	x	x	x	x
1150		x		x
1200	x	x	x	x
1250	x		x	
1300	x	x	x	x
1350		x		x
1400		x		x

4.5　Velocity measurements in bend

Measurement of the velocity after the bend is shown on figure 4.8 and 4.9. The pitot tube has three pressure holes; the centre hole measures stagnation pressure and the holes on each side measure hydraulic pressure. The height difference of the water columns are levelled and measured.

Measurements are done on 3.5 and 5 meter pressure head, and on the rotational speeds 400, 800 and 1300 rpm. These are the minimum, best operation and maximum rotational speeds, respectively. Measurements are not done with a pressure head of 5 meters on 1300 rpm because of overheating of the upper bearing. All the measurements are done on runner vane setting 2.

Figure 4.8: Pitot tube

Figure 4.9: Measuring pressure difference

4.6 Risk assessment

Working in a laboratory there is potential risk to human or environment related to the test rig. NTNU requires that a risk assessment is carried out for all students working in a laboratory. A yellow card and a green card is issued by the institute and has to be available at the test rig at all times. This is shown in figure 4.10. The risk assessment is included in appendix F.

Figure 4.10: Yellow and green card

Chapter 5

Uncertainty analysis

All measurements have errors, both systematic and random. How to accomplish an error analysis is described in IEC (IEC, 1999, ch 3.9). An error, e_x, is defined as "the difference between the measurement and the true value of the quantity". Uncertainty, f_x, is defined as "the range within which the true value of a measured quantity can be expected to lie, with a suitably high probability". A 95% confidence level is chosen. To combine uncertainties, equations (5.1) to (5.4) are used.

$$f_x = \frac{e_x}{x} \tag{5.1}$$

$$f_{x^n} = n \cdot f_x \tag{5.2}$$

$$f_{xy} = \sqrt{f_x^2 + f_y^2} \tag{5.3}$$

$$f_{x+y} = \frac{\sqrt{e_x^2 + e_y^2}}{x + y} \tag{5.4}$$

The uncertainty is calculated for best efficiency point at setting 1, with the test-results from 5 meters pressure head, and for best efficiency point at setting 2, with a pressure head of 3.5 meters. The uncertainties are calculated in Matlab and Excel, and the calculations can be found in appendix C.

5.1   Types of errors

Spurious errors are errors that invalidate a measurement. These can be human errors or instrument malfunction. Spurious errors should not occur, and measure-

ments with spurious errors should be discarded and repeated without spurious errors.

Random errors, e_r, are small deviations in measurements done with the same input caused by numerous small independent influences in the instrumentation and operating condition. The measurements will normally form a normal distribution when doing several measurements.

The random error can by found by equation (5.5) where n is the number of measurements, t is the Student's coefficient for (n-1) degrees of freedom given in table L.2 in IEC (IEC, 1999, p.549), and s_x is the standard deviation given by equation (5.6).

$$e_x = \pm \frac{t \cdot s_x}{\sqrt{n}} \tag{5.5}$$

$$s_x = \sqrt{\frac{\sum (\overline{x} - x_i]^2}{n-1}} \tag{5.6}$$

In equation (5.6) $\overline{x}$ is the mean value of the measurements and x_i is the value of measurement i.

Systematic errors, e_s, are errors due to uncertainties in the equipment and will not change while doing several measurements. Systematic errors can be measured by doing the same measurements with two different instruments, or by judging the uncertainty in the equipment involved.

The **total uncertainty** (f_t) is given by combining the systematic (f_s) and random (f_r) uncertainty in a 95% confidence interval, given by the root-sum-squares method shown in equation (5.7).

$$f_t = \pm \sqrt{f_r^2 + f_s^2} \tag{5.7}$$

5.2   Uncertainty in calibrations

The calibration certificate for the constant of gravity is attached in appendix B.4. The uncertainty is very small, and is therefore neglected in the rest of the uncertainty analysis.

In calibration of the instruments there are random errors in the measurements and systematic errors in the equipment used. The random error is given in the calibration reports found in appendix B.1, B.2 and B.3. The random error will vary for each measurement, and follow a second order equation. In the following sections, the random error is given for the best efficiency point.

Torque transducer

The dish and wire are weighed with an error of 0.05 g. The moment arm is the sum of the radius of the shaft and the additional arm, with errors of respectively 0.1 mm and 1 mm. The weights used have an uncertainty of 0.15 g for the 5 kg weights and 0.065 g for 2 kg, given in appendix B.1. The systematic uncertainty for the torque transducer at the best efficiency point is given in equation (5.8).

$$f_{T,s} = \pm\sqrt{f_m^2 + f_g^2 + f_{arm}^2} = \pm\sqrt{0.0011^2 + 0.1927^2} = \pm 0.1927\% \qquad (5.8)$$

At best efficiency point at setting 1, the torque is 148.1934 Nm, with a random uncertainty of 0.2265 % from the calibration report.

The total uncertainty for the torque is given in equation (5.9).

$$f_{T,t} = \pm\sqrt{f_s^2 + f_r^2} = \pm\sqrt{0.1927^2 + 0.2265^2} = \pm 0.2974\% \qquad (5.9)$$

Pressure transducer

The primary calibrator of the pressure transducer has a systematic uncertainty shown in appendix B.2 of 0.0001 %. At best efficiency point, the inlet pressure is 0.493 bar, with a random uncertainty of 0.0527 %.

The total uncertainty for the inlet pressure is given in equation (5.10).

$$f_{p_1,r} = \pm\sqrt{f_s^2 + f_r^2} = \pm\sqrt{0.0001^2 + 0.0527^2} = \pm 0.0527\% \qquad (5.10)$$

Trip meter

The systematic error in the trip meter is 0.5 rpm. At best efficiency point, the rotational speed is 949.836 rpm, with a random uncertainty of 0.1211 %.

The total uncertainty for the trip meter is given in equation (5.11).

$$f_{n,r} = \pm\sqrt{f_s^2 + f_r^2} = \pm\sqrt{0.0526^2 + 0.1211^2} = \pm 0.1321\% \qquad (5.11)$$

Volume flow

Calibration of the flow meter was done by Stople (Stople, 2011, Annex C). The uncertainty at best efficiency point is 0.0978 %.

Water temperature and atmospheric pressure

The atmospheric pressure and water temperature are constantly measured in the laboratory, and the calibration certificates are attached in appendix B.5. The water temperature and atmospheric pressure has a total uncertainty of 0.03 % and 0.05 %, respectively.

5.3   Uncertainty in tests

The random uncertainties in the tests are calculated in Matlab from the registered raw data for the best efficiency point. The equations for random errors given in chapter 5.1 are used. The total uncertainties for the calibrations are shown in table 5.1.

Table 5.1: Total uncertainty in calibrations, setting 1

	Test $\mathbf{f}_{test}$	**Calibration** $\mathbf{f}_{cal}$	**Total** $\mathbf{f}_{total}$
T	0.0048 %	0.2974 %	**0.2974 %**
p_1	0.1119 %	0.0527 %	**0.1237 %**
n	0.0016 %	0.1321 %	**0.1321 %**
Q	0.0035 %	0.0978 %	**0.0979 %**

5.4   Uncertainty in calculations

The water density, outlet pressure, effective pressure head and hydraulic efficiency are calculated values.

The water density is a function of the atmospheric pressure and the water temperature, both with small uncertainties. An uncertainty analysis was done in the laboratory by Pål Tore Storli (Storli, 2006) giving an uncertainty of 0.01 %.

Outlet pressure

The uncertainty in outlet pressure, p_2, is given by equation (5.12) with the velocity uncertainty given in equation (5.13). The pipe radius is assumed to have an error of 0.1 mm. The tail water height, $p_{s,2}$ is measured to be 51 cm with an uncertainty of 2 cm.

$$f_{p2} = \frac{\sqrt{e_{p_{s,2}}^2 + (\frac{e_{v22}}{2g})^2}}{p_{s,2} - \frac{v_2^2}{2g}} \quad \text{where} \quad e_{v^2} = 2 \cdot v^2 \cdot f_v \tag{5.12}$$

$$f_v = \pm\sqrt{f_Q^2 + 2f_r^2} \quad \text{where} \quad v = \frac{Q}{A} = \frac{Q}{\pi r^2} \tag{5.13}$$

Solving equation (5.12) and (5.13), an uncertainty of 4.2822 % is obtained.

Effective pressure head

The total uncertainty in effective pressure head is given in equation (5.14).

$$f_{H_e,t} = \pm\frac{\sqrt{(\frac{e_{p_1}}{\rho g})^2 + (\frac{e_{p_2}}{\rho g})^2 + (\frac{e_{v1^2}}{2g})^2 + (\frac{e_{v2^2}}{2g})^2 + (e_z)^2}}{\frac{p_1 - p_2}{\rho g} + \frac{v_1^2 - v_2^2}{2g} + z} \tag{5.14}$$

The uncertainties for ρ and g are neglected in this calculation. The distance between the inlet and outlet, z, is measured with an uncertainty of 2 mm.

The uncertainty in H_e is calculated to be 0.3060 %.

Hydraulic efficiency

The hydraulic efficiency is a function of the parameters torque, rotational speed, water density, volume flow, constant of gravity and pressure head as shown in equation (2.6). The root-sum-square-method is used to combine the uncertainties in all components to give the total uncertainty in efficiency for setting 1, given in equation (5.15).

$$\begin{aligned} f_\eta &= \pm\sqrt{f_T^2 + f_n^2 + f_\rho^2 + f_Q^2 + f_g^2 + f_{H_e}^2} \\ &= \pm\sqrt{0.2974^2 + 0.1321^2 + 0.01^2 + 0.0979^2 + 0.3060^2} \\ &= \pm 0.4574\% \approx \pm 0.46\% \end{aligned} \tag{5.15}$$

5.5 Calculation of uncertainty, setting 2

The uncertainty in calibration and tests at best efficiency point, setting 2, is showed in table 5.2.

Table 5.2: Total uncertainty in measured values, setting 2

	Test $\mathbf{f}_{test}$	Calibration $\mathbf{f}_{cal}$	Total $\mathbf{f}_{total}$
T	0.0037 %	0.2620 %	**0.2621 %**
p_1	0.1286 %	0.0872 %	**0.1554 %**
n	0.0016 %	0.1622 %	**0.1622 %**
Q	0.0024 %	0.0978 %	**0.0978 %**

The outlet pressure is calculated to have an uncertainty of 4.4776 %, the effective pressure head has an uncertainty of 0.3864 %, and the total uncertainty for best efficiency point, setting 2, is 0.5039 % $\approx$ 0.50 %.

Chapter 6

Simulations of the turbine inlet

Computational fluid dynamics (CFD) is a simulation tool that is widely used because of its low cost compared to doing tests in a laboratory. The CFD program Ansys Fluent is used to simulate the flow in the bend just before the turbine. It is important to keep in mind that even though the results look right, the solution should be compared to known test results.

6.1   Original geometry

The Afghanistan turbine has been drawn in Inventor by Anders Austegård. Autodesk Inventor Professional 2011 is a computer-aided design (CAD) software for mechanical 3D design. The geometry made for the simulation is based on Austegård's drawings, with the same measurements.

When saving design from Inventor as a .stp file it can be directly imported to Design Modeller in Ansys. The original geometry with two flow controllers is shown in figure 6.1. The inlet and outlet has been extended in order to obtain uniform velocity in the inlet, and prevent backflow in the outlet.
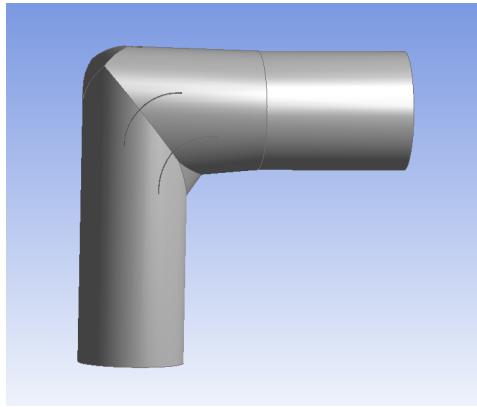
Figure 6.1: The original bend geometry

6.2   Grid

The grid is an unstructured, tetrahedron grid made in the patch conforming al-
gorithm in the mesh program in Ansys. All walls, including the shaft, has been
inflated, and an additional face sizing is chosen on both flow controllers in order
to get a smooth grid close to the walls. The refinements around the flow controller
and shaft is shown in figure 6.2. The original geometry mesh contains 533,578
nodes and 1,488,794 elements. Some statistics are shown in table 6.1.
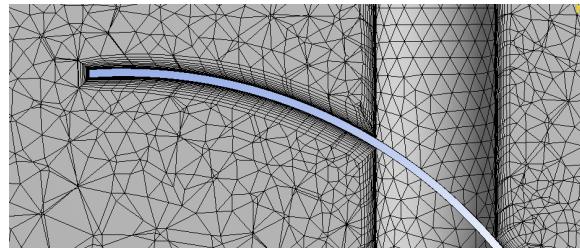
Figure 6.2: The grid has been refined around the walls

Table 6.1: Grid statistics

	Min	**Max**	**Average**
Orthogonal quality	0.11	1	0.89
Skewness	1.93 E-4	0.9	0.20
Aspect ratio	1.16	154.82	13.60
y+ value	1.11	22.41	

The orthogonal quality is number between 0 and 1, where a value close to 1 is the best (Ansys, 2012, ch.13.2.1). The minimum orthogonal quality should not be less than 0.01, and the average value should be significantly higher. An average of 0.89 is satisfying.

The skewness is a number between 0 and 1, where a value close to 0 is best. If a cell has high skewness it can decrease the accuracy and destabilise the solution, or never converge. The maximum skewness should not be more than 0.95 for a tetrahedral mesh, and the average value should be significantly lower. A average skewness of 0.20 is good.

The aspect ratio is the ratio between the length and the height of a node. A low aspect ratio is necessary for the solution to converge and sudden or large changes in the aspect ratio should be avoided. This grid has a average aspect ratio of 13.60.

It is important to keep a smooth grid close to the wall, because of the boundary layer effect on the flow. The y+ value is a measurement of the effect of the boundary layer, and should be kept as low as possible. The boundary layer should have at least ten cells normal to the layer. All walls in this mesh has a refinement of 12 cells.

The geometry is divided into *velocity-inlet*, *outflow*, *wall* and *rotating wall* in the mesh program.

6.3   Boundary conditions

The boundary conditions for simulations done at 800rpm are shown in table 6.2. Simulations are done from the velocity inlet, with a temperature of 20 °C.

Table 6.2: Boundary conditions at 800 rpm, setting 2

	Boundary Condition	**Comment**
Velocity inlet		
Inlet velocity	3.11 m/s	Q/A
Initial gauge pressure	35 000 Pa	3.5 m pressure head
Turbulent kinetic energy (k)	0.011 m^2/s^2	
Specific dissipation rate (ω)	6.84 1/s	
Outflow	1	No loss of mass
Wall		
Roughness constant	0.5	No slip, stationary
Rotating wall		
Roughness constant	0.5	No slip, rotational
Speed	136.2 rad/s	800rpm

The turbulent kinetic energy (k) and specific dissipation rate (ω) are given by equations (6.1) and (6.2) (Ansys, 2012, ch.7.3.2).

$$k = \frac{3}{2} \cdot (v \cdot I)^2 \quad \text{where} \quad I = 0.16(Re)^{-1/8} \tag{6.1}$$

$$\omega = \frac{\sqrt{k}}{0.09^{1/4} \cdot 0.07 \cdot D} \tag{6.2}$$

6.4   Solution method and post processing

The k-ω turbulence model is chosen, because this is a good model to simulate boundary layer flow and separation (Ansys, 2012, ch.13.2.1). It is sensitive to the values of k and ω outside the shear layer, and the SST (shear-stress transport) model has therefore been designed. SST-k-ω computes flow separation and wall boundary layer characteristics accurately, and it is one of the most widely used models for aerodynamic flows. Enhanced wall treatment is default.

The chosen solution method is SIMPLE, first order upwind with a pressure based solver.

Residual is the difference between the iterated value and exact solution. In Fluent it is the difference between two iterations, and the solutions should converge with residuals of 10^{-4} for the velocity and 10^{-5} for the continuity.

Post processing of the results is done in CFD-Post, where the velocity contour in the mid plane through the bend is presented. The velocity profiles are plotted in the Solution program in Fluent.

Chapter 7

Results

7.1 Efficiency test

Tests have been done on runner vane setting 1 and 2, on 3.5 and 5 meter pressure head. The results are presented as reduced parameters, n_{ed} and Q_{ed}.

Because tests were only done on runner vane setting 1 and 2, a general Hill diagram has not been made.

7.1.1 Best efficiency point

The test results with the best efficiency for setting 1 and 2 are presented in table 7.1, and graphically in figure 7.1 and 7.2. Setting 2 gives a higher efficiency because the volume flow increases with the runner vane opening. The volume flow also increases with the rotational speed, as can be seen in figure 7.2.

Figure 7.1: Efficiency diagram
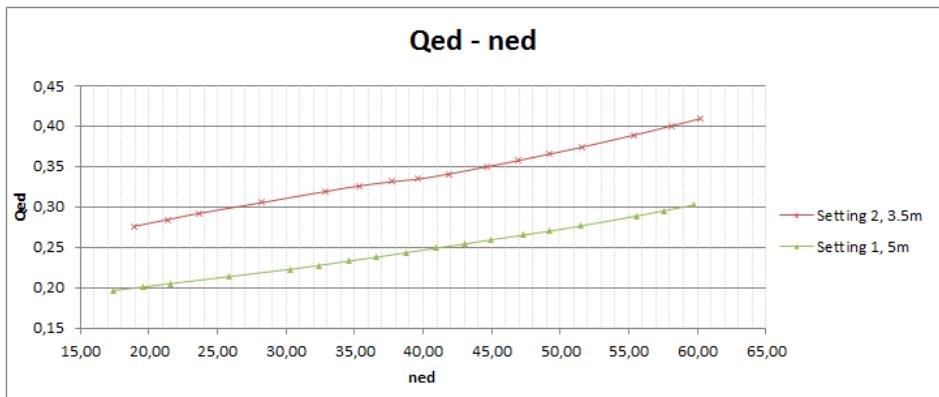
Figure 7.2: Qed ned

The uncertainty at best efficiency point is calculated to be 0.46 % at setting 1, and 0.50 % at setting 2.

Table 7.1: Test results at best efficiency point, setting 1 and 2

	Setting 1	Setting 2
n	949.84 rpm	799.07 rpm
n_{ed}	40.91	37.72
η	85.32 %	87.75 %
h	5.03 m	3.44 m
H_e	6.88 m	5.73 m
Q	256.24 L/s	311.14 L/s
Q_{ed}	0.2431	0.3311
P_1	0.4931 bar	0.3369 bar
P_2	0.4671 m	0.1066 m
P_{atm}	99.92 kPa	100.99 kPa
T	148.19 Nm	183.16 Nm
ρ	998.14 kg/m^3	998.23 kg/m^3
θ	20.58 °C	20.15 °C

For a rotational speed of 800 rpm at setting 1, the efficiency and volume flow as a function of the effective pressure head is shown in figure 7.3. In appendix D the results at 800 rpm at setting 1 are compared to the results at 800 rpm, setting 2.
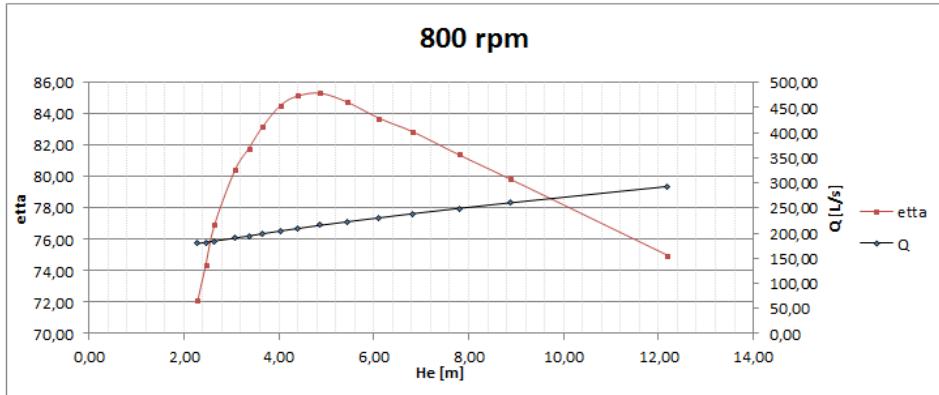
Figure 7.3: Efficiency at 800 rpm (setting 1)

7.1.2 Tests done on different pressure heads

Because reduced parameters are used, the efficiency curves should be the same no matter which pressure head is used. Still, all measurements have uncertainties and some variations in the measurements can be expected even though they are done

under the same external conditions. Measurements on 3.5 and 5 meter pressure
head for runner vane setting 1 and 2 are shown in figure 7.4 and 7.5, respectively.
Even though they are similar, the variations between the efficiency curves at 3.5
and 5 meter pressure head are higher than the calculated uncertainty and must be
caused by other relations.
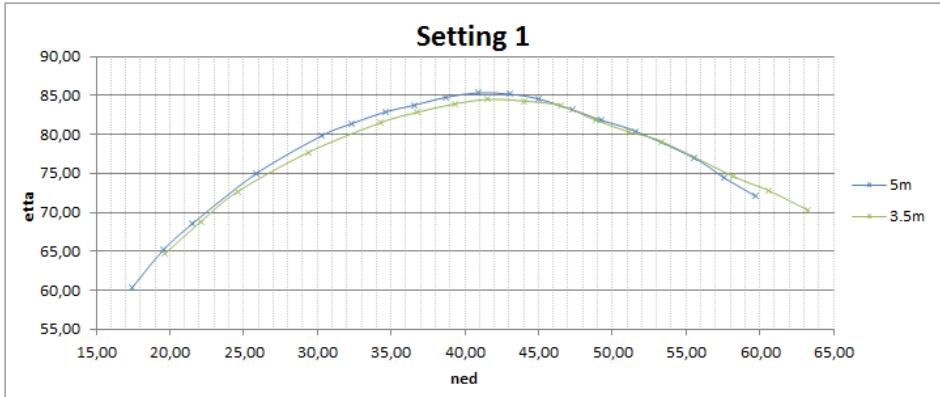
Figure 7.4: Measurements done on setting 1, pressure head 3.5 and 5 m
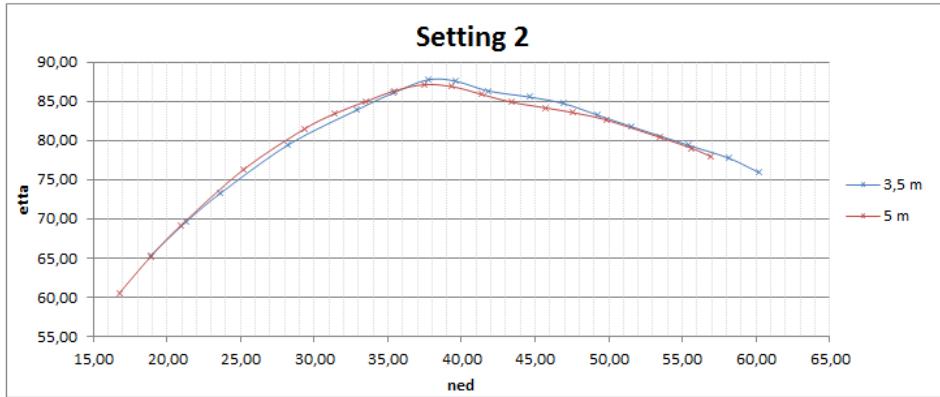
Figure 7.5: Measurements done on setting 2, pressure head 3.5 and 5 m

7.1.3   Repeated measurements after moving the runner vanes

On runner vane setting 1, tests were done both before and after the runner vanes
were changed to setting 2. The test results are shown in figures 7.6 and 7.7.
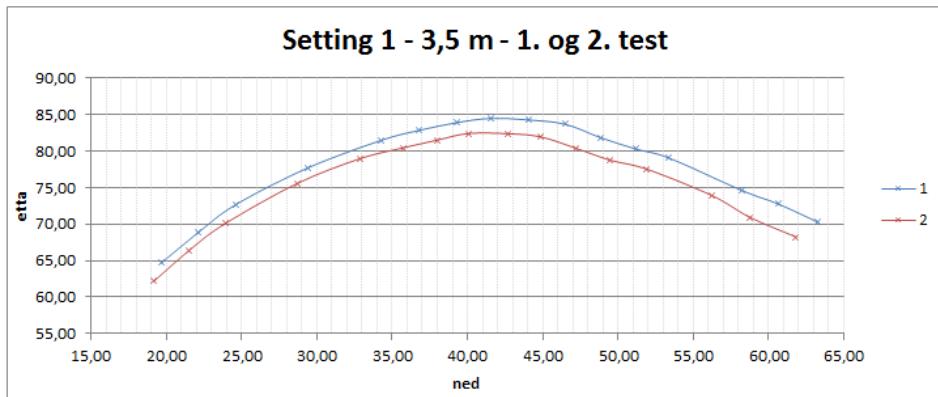
Figure 7.6: Measurements done on setting 1
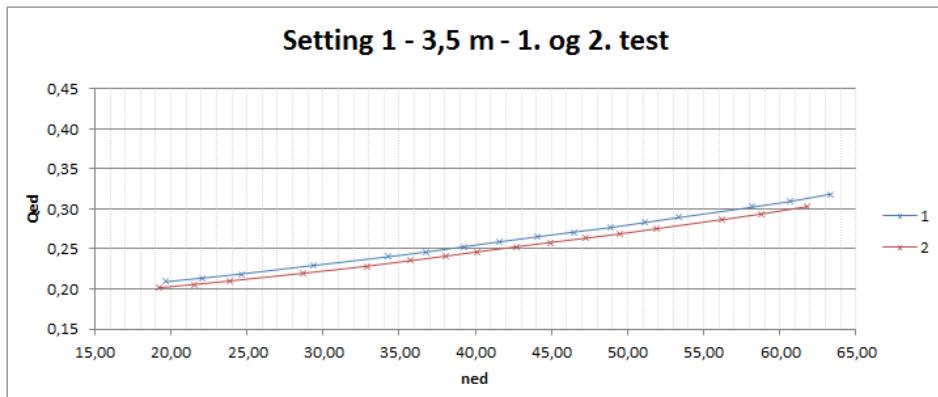
Figure 7.7: Measurements done on setting 1, Q_{ed} - n_{ed}

The volume flow is higher in the first test than in the second, giving a higher efficiency. It is probable that this is because the runner vanes are not placed in the exact same position.

7.2 Improvements of 90 degree bend

The 90 degree bend has been simulated in Fluent, and the simulation results from the original geometry has been compared to results from Pitot measurements done in the laboratory.

7.2.1   Simulations

All simulations are done with boundary conditions (inlet velocity, rotational speed and Reynolds number) for setting 2 with a pressure head of 3.5 meter. Setting 2 has a higher volume flow than setting 1 and it is therefore more likely that the negative effects of the 90 degree bend are higher at setting 2. The velocity in the mid cross section of the bend is presented in the figures. Describing the simulations, the expressions *inner* and *outer* part of the bend and pipe are used. The inner and outer part of the bend is where the curvature is highest and smallest, respectively, and the inner and outer part of the pipe is the elongation of the bend, respectively.

The velocity profiles are given in the same cross section as in the contour figures, but in the inlet to the turbine. The zero-point of the x-axis is the center of the pipe where the shaft is placed, and the velocity is therefore zero.

All solutions converged with residuals of 10^{-4} for velocity, k and ω and 10^{-5} for the continuity. This is shown in figure 7.8, for the simulation done on the original geometry at 800 rpm.
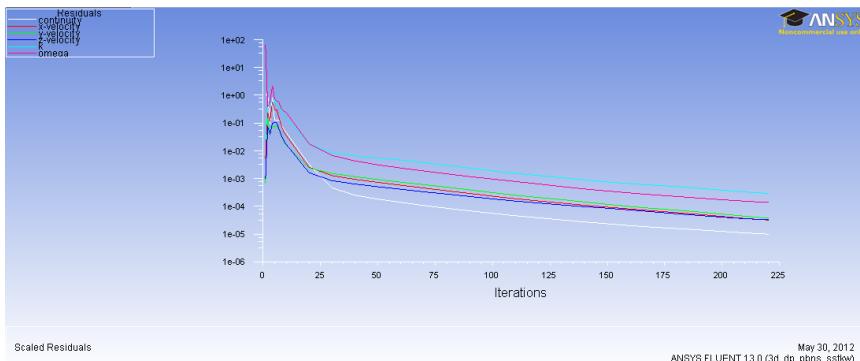
Figure 7.8: Residuals at 800 rpm, original geometry

Original geometry

Results from simulations done on the original geometry, are showed in figure 7.9 for rotational speeds of 400, 800 and 1300 rpm respectively. A higher rotational speed increases the volume flow, and velocity. In the outlet of the bend, the velocity is higher in the outer part, than in the inner part of the pipe. The inner part has a remarkable drop in the velocity caused by the inner rounding of the bend.
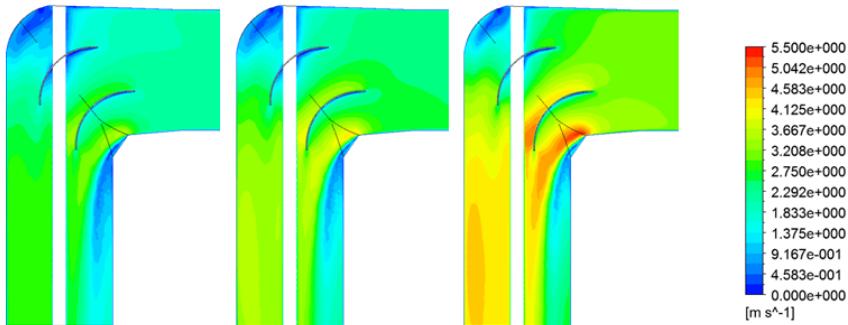
Figure 7.9: Original geometry - 400, 800 and 1300 rpm

Figure 7.10 shows the velocity profile into the turbine for 400, 800 and 1300 rpm. The figure shows that even though the velocity increases, the velocity profile into the turbine is the same.
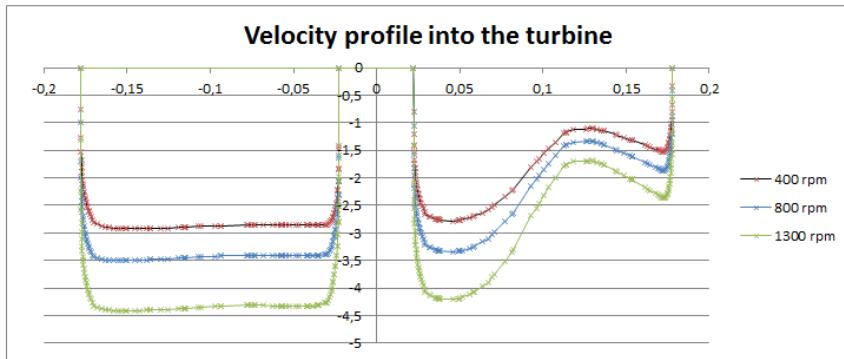
Figure 7.10: Velocity profile - 400, 800 and 1300 rpm

Bend with zero, one and two flow controllers

To check if the flow controllers have positive effect on the fluid flow, the bend has been simulated without and with only one flow controller, and the simulation results are shown in figure 7.11. The result on two flow controllers in figure 7.11 is the same as the one on 800 rpm in figure 7.9, but with different scaling on the velocity.
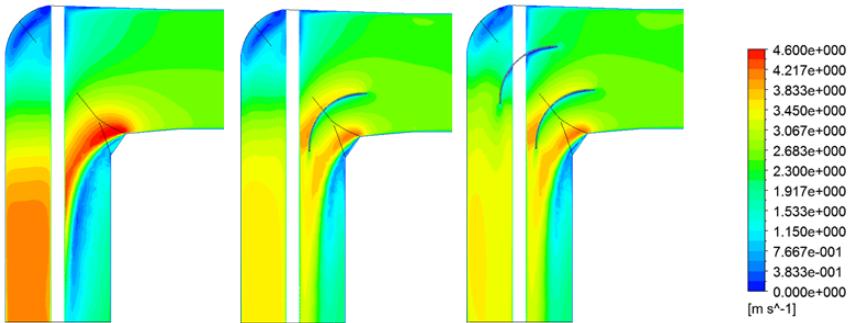
Figure 7.11: 800 rpm - zero, one and two flow controllers

Figure 7.12 shows the velocity profile into the turbine at 800 rpm, with two, one and zero flow controllers. The figure shows that the flow controllers have a highly positive effect on the flow, but that the upper flow controller does not have much additional effect, compared to only one flow controller. In further simulations, the upper flow controller has been removed.
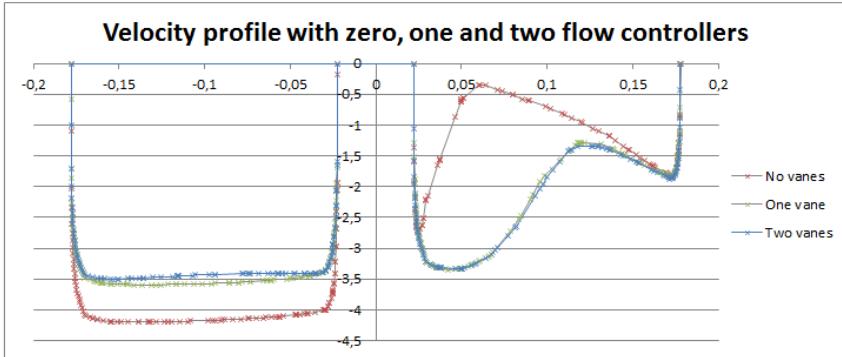
Figure 7.12: Velocity profile - zero, one and two flow controllers

One flow controller moved to the right

In order to accelerate the fluid velocity in the inner part, the flow controller is moved to the right. This gives a higher volume flow under the flow controller, and will accelerate the flow in the flow controller outlet, where the cross section area is smaller. In figure 7.13 the flow controller is moved 2 and 5 cm to the right, respectively. Moving the flow controller more than 5 cm, it will be in conflict with the inner rounding of the bend.
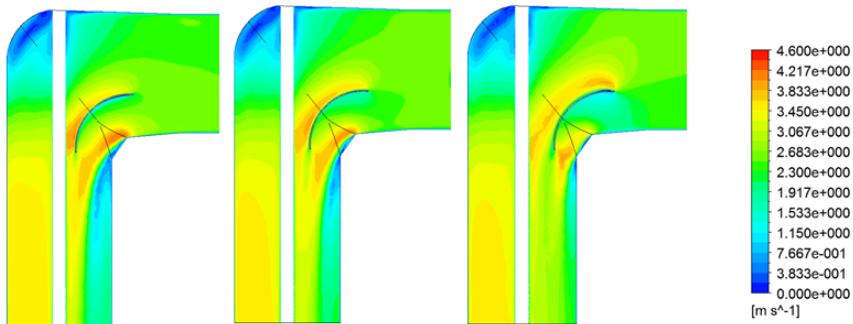
Figure 7.13: One vane - moved 2 and 5 cm to the right, respectively

Figure 7.14 shows the velocity profile into the turbine at 800 rpm with one flow controller, where the flow controller has been moved to the right. Moving the flow controller shows a positive effect on the flow.
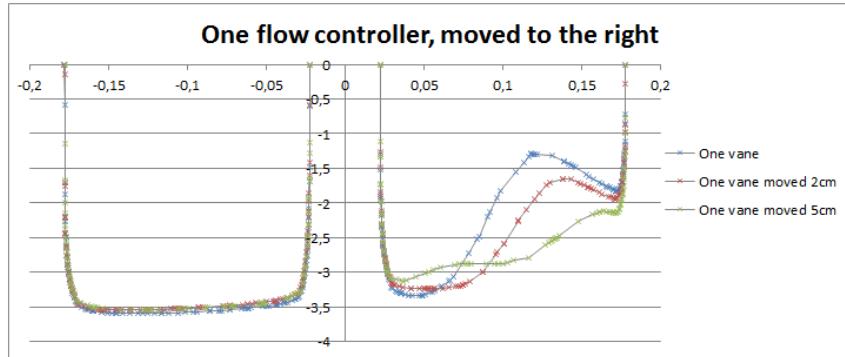
Figure 7.14: Velocity profile - one vane moved 2 and 5 cm

Flow into the turbine

The velocity in a cross section area just before the turbine is shown in figure 7.15, seen from above. The figure shows the flow with the original geometry, one flow controller originally placed and one flow controller moved 5 cm to the right. In the original geometry, there is a remarkable area with very low velocity. This area is not that remarkable when the flow controller has been moved, but even though the flow has been improved, it is still not optimal.
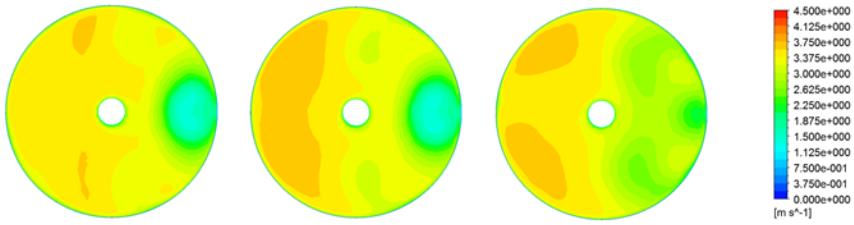
Figure 7.15: Flow into the turbine - original geometry, one flow controller originally placed, one flow controller moved 5 cm to the right

7.2.2   Pitot measurements

To check if the simulation results are correct, Pitot measurements have been done in the laboratory. The measurements have been done in the inner part of the pipe approximately 20 cm beneath the inner rounding of the bend and with a small angle from to the mid plane. The measured height difference between the static pressure and the stagnation pressure is shown in table 7.2.

Table 7.2: Pitot measurements in laboratory, measured values Δh in cm

Rotational speed [rpm]	Pressure head [m]	From shaft [cm]				
		1	3	5	7	9
400	3.5	47	40	26	10	16.5
		47	37.5	18	10	18.5
		47	38.5	23	10.5	21.5
	5	54	46.5	36	14	24
		54	45.5	22.5	12.5	25
		55	47.5	26	13	24.5
800	3.5	71	59	33	13	32
		70	58	27	13	32
		70	59	30	14	33
	5	78	66	36	16	42
		77	64	27	15	42
		78	69	34	15	40
1300	3.5	118	102	44	20	54
		118	100	37	23	55

The measurements show the same drop in velocity near the inner wall as shown in the simulations. By increasing the volume flow (rotational speed), the velocity increases, but the largest increase is close to the shaft and the wall. Three series of

measurements are done for all conditions, except for at 1300 rpm, where the upper bearing got to warm to continue. The highest uncertainties in the measurements are between the drop and the shaft.

The velocities in figure 7.16 are calculated from equation (2.11). The graph shows the absolute velocity in the inner part of the pipe, from the shaft to the wall.
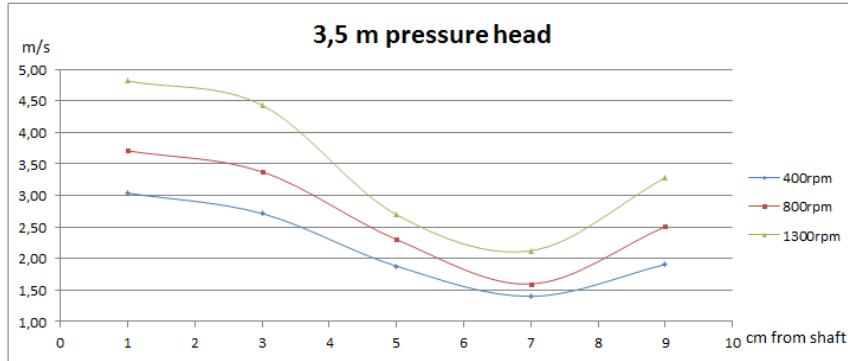
Figure 7.16: Pitot measurements, constant pressure head 3.5m

Increasing the pressure head to 5 meter, the velocity profile stays the same but with the largest increase in velocity close to the shaft and the wall, as for the increase of rotational speed, and a smaller increase at the drop. This is shown in figure 7.17.
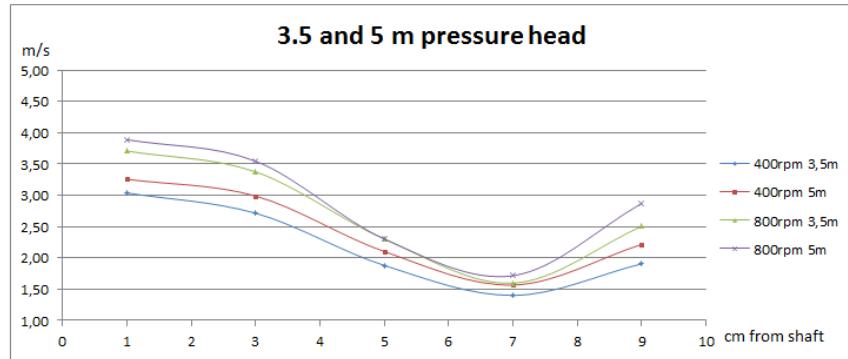
Figure 7.17: Pitot measurements

7.2.3 Simulations compared to Pitot measurements

Figure 7.18 show the Pitot measurements at 3.5 meter pressure head, compared to the simulations at the original geometry. The measurements show the same drop

in velocity that can be seen in the simulations. Close to the shaft, the measured
values are higher than for the simulations.
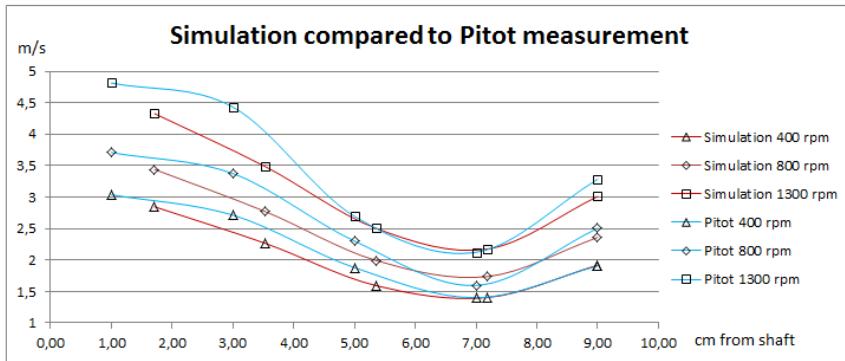
Figure 7.18: Simulations compared to Pitot measurements

Chapter 8

Discussion

8.1 Efficiency

A Hill diagram presents efficiencies at increasing dimensionless rotational speed and volume flow, at different runner vane angles. Because tests were only done on two different runner vane angles, a Hill diagram would not be a good way to present the results, and they were therefore presented as n_{ed} - Q_{ed} and η - n_{ed} graphs.

Best efficiency point for runner vane setting 1 and 2 are given in table 8.1.

Table 8.1: Best efficiency point, setting 1 and 2

	Setting 1	Setting 2
η	$85.31859 \pm 0.46\,\%$	$87.749456 \pm 0.50\,\%$
n_{ed}	40.9108	37.7203
Q_{ed}	0.2431	0.3311

The best efficiency was found for setting 1 at 5 meter pressure head, and for setting 2 at 3.5 meter pressure head.

Using reduced parameters, the efficiency curves should be the same no matter which pressure head is used. Measurements done on two different pressure heads give similar results but the variations are not covered by the $0.5\,\%$ uncertainty, even though the measurements are done for the same external conditions. Because the Reynolds number will increase with increased pressure head, the efficiency will be slightly increased because of reduction in friction loss (from the Moody diagram)

at higher pressure heads. At setting 1 the best efficiency was found for 5 meter pressure head.

At setting 2, on the other hand, best efficiency was found on 3.5 meter pressure head. This is not according to the Reynolds number theory. One explanation can be that the decrease of efficiency in higher pressure head is caused by the bend. A higher pressure head gives a higher volume flow into the bend. The velocity profile will be more unevenly distributed into the turbine than for a lower pressure head and the flow disturbance will reduce the efficiency. This effect can be greater than the effect of higher Reynolds number, and give a lower efficiency for higher pressure head at high volume flows.

From the reduced parameters n_{ed} and Q_{ed}, best efficiency point for the preferred operation point (pressure head or rotational speed) can be found.

Stople and Fjærvold got a best efficiency of 76.4 % and 83.9 % at runner vane setting 1 and 2, respectively, with an uncertainty of 1.58 %. They concluded that the best efficiency point was not found, because of restrictions in the measurements done. The best efficiency points found in this thesis are high taking the condition of the turbine into consideration, but compared to what Stople and Fjærvold found, they are not unlikely.

The uncertainty is calculated to be 0.5 % at best efficiency point. This is where the uncertainty is smallest. In the laboratory at NTNU the uncertainty of the measurements should be less than 0.2 %. Taking the condition of the turbine into consideration, an uncertainty of 0.5 % is satisfying. In the tests, the random uncertainty is highest for the pressure head measurements. Water is pumped through a pressure tank, and because of the constant oscillations in the water it is difficult to keep the head constant. The systematic error in the calibrations is highest for the calibration of the torque.

To change the runner vane settings is difficult and takes a lot of patience, because of the placing of the turbine inside a pipe with access only from above and below the turbine. The settings are marked as small indents where the vane is attached, and it is impossible to move it back to the exact same point once moved. When running the same tests after moving the runner vanes, variations in the results will occur. Increase of the runner vane opening or the rotational speed, increases the volume flow.

8.2   Improvements of 90 degree bend

A 90 degree bend creates disturbance to the fluid flow. It is desirable that the flow into the turbine is more or less uniform, and a 90 degree bend just before the turbine is not recommended. Nevertheless, use of flow controllers helps normalise the flow, compared to no controllers.

Increasing the rotational speed of the turbine, increases the volume flow. It is

found that even though the fluid flow increases, the flow profile in the bend will be similar, but that the difference between the highest and lowest velocity will be higher. The velocity is low in the inner part of the bend with a significant drop in velocity close to the wall, and high in the outer part, giving an uneven velocity profile in a cross section area.

The inner rounding creates separation and the flow does not follow the geometry. The flow will continue to the outer part of the pipe and create a high velocity in the outer part, and an area close to the inner wall where the velocity is close to zero. This area is decreased by flow controllers, and even more decreased by moving the lower flow controller to the right. According to theory, a higher pressure in the outer part caused by the volume flow, will decrease the pressure in the inner part, and therefore increase the velocity (according to Bernoulli's equation). This tendency is not seen in the simulations or measurements.

The turbine as it is today, has two flow controllers placed in the bend, in addition to the outer and inner rounding of the bend. Simulations show that the upper flow controller does not have much effect on the flow, and it can therefore be removed. The lower flow controller helps distribute the flow better compared to zero flow controllers, giving a higher velocity in the inner part of the pipe and reducing the velocity in the outer part. The drop in velocity is also highly reduced. Moving the flow controller to the right leads more flow through the inner part of the bend, and reduces the drop even more. The velocity profile into the turbine is still not optimal when the flow controller has been moved, but better than with the geometry as it is today.

In the turbine system there are guide vanes to lead the flow into the turbine in a more efficient way. These guide vanes will help give a more even distribution of the flow into the turbine, but with the big velocity variations as seen in the simulations and Pitot measurements, the flow into the turbine will still have great variation, and this will decrease the efficiency compared to having a uniform flow into the turbine.

The Pitot measurements done in the laboratory confirm that there is a big drop in the velocity between the shaft and the wall in the inner part of the pipe. Between the drop and the shaft, the Pitot measurements give higher values than the simulation. Pitot measurements done with increased rotational speed and pressure head, show the same tendencies in the velocity profile, with a drop close to the inner wall, and higher velocity close to the shaft.

A more even velocity profile after the bend will give higher efficiency and is therefore preferable.

Chapter 9

Conclusion and further work

This turbine is made in Afghanistan, and it is desirable that the construction is non-complex in order to make and maintain the turbine in a village, giving the inhabitants the feeling of "ownership" and willingness to run and maintain the turbine. The turbine system has a 90 degree bend with two flow controllers, before the non adjustable guide vanes and the runner. The runner vanes have four positions that is adjusted by hand, depending on the volume flow and pressure head accessible. Setting 1 gives the lowest volume flow. The volume flow is also increased by the rotational speed of the turbine.

The runner is constructed to fit in the turbine housing at setting 1, but changing to setting 2, 3 and 4 it has to be "self-grinded" in order to fit in the housing. This is done in order to make the gap between the turbine and the housing as small as possible. The self-grinding process has been done for setting 1 and 2, but at setting 3 the runner was completely stuck in the housing, making it impossible to turn. It was suggested by Austegård to move the turbine further up in the housing, but this was considered to take too much time because the whole turbine system would have to be taken apart and assembled again. Complete tests has been done on runner vane setting 1 and 2.

The best efficiency was found to be 85.32 % at runner vane setting 1, and 87.75 % at runner vane setting 2, with an uncertainty of 0.5 %. The results has been presented with reduced parameters, and best operation point for the desired operation condition can be found from these results. It should be kept in mind that a higher pressure head gives a higher Reynolds number and reduced friction loss according to the Moody diagram. A higher efficiency can therefore be obtained for higher pressure heads. This effect seems to be repealed by the additional loss in the bend at high volume flow, making the disturbance of the velocity profile into the turbine even more significant, and decreasing the efficiency.

Simulations show that the upper flow controller in the bend does not have much, if any, effect on the flow, but that the lower flow controller help distribute the flow in

a significantly better way. Moving the lower flow controller to the right, will help distribute the flow even better. This will increase the efficiency of the turbine.

Working on this turbine has been challenging because of the lack of easy access to the turbine runner. It takes a lot of time and patience moving the runner vanes, and the indents makes it impossible to move the vanes to the exact same position once moved. The upper bearing gets overheated when running on high rotational speeds. It is likely that this is caused by vibrations in the shaft caused by the uneven velocity profile.

Taking the condition of the turbine, and the simplified construction, into consideration, the turbine has a high efficiency.

Future work

- Efficiency tests should be done for runner vane setting 3 and 4 and a complete Hill diagram should be made

- The turbine design should be changed, so that runner vane angles can be changed in an easier way

- The lower flow controller should be moved to the right in order to give a better velocity profile into the turbine, and the upper flow controller can be removed

- The self-grinding process should be reconsidered, making the turbine fit the housing in a better way

- Cavitation has not been looked at in this thesis. It is likely that improving the volume flow conditions in the bend, will reduce the cavitation problems in the turbine system. This should be confirmed, doing tests on an improved geometry

References

AEIC, 2012. *Afghan Energy Information Center.* [online].
Available at: <http://afghaneic.org/index.php> [Accessed March 2012]

Ansys, 2012. *Ansys Fluent User's Guide.* [online].
Available at: <http://ansys.com/> [Accessed February to June 2012]

Brekke, H., 2000. *Grunnkurs i hydrauliske Strømningsmaskiner*
Trondheim: Vannkraftlaboratoriet NTNU

Brekke, H., 2003. *Pumper & Turbiner*
Trondheim: Vannkraftlaboratoriet NTNU

Dahlhaug, O.G., 2012. *Lectures in TEP4195 Turbomaskiner.* [Power Point presentations] (Lectures, spring 2012)

Fjærvold, L., 2011. *Improvements of a Kaplan type small turbine*
Master thesis. Norwegian University of Science and Technology.

International Electrotechnical Commission, NEK IEC 60193, 1999.
Hydraulic turbines, storage pumps and pump-turbines. Model acceptance tests
2nd ed.

Remote HydroLight, 2012. *Remote HydroLight.* [online].
Available at: <http://www.remotehydrolight.com/index.html> [Accessed March 2012]

Stople, R.A., 2011. *Testing efficiency and characteristics of a Kaplan-type small turbine*

Project thesis. Norwegian University of Science and Technology.

Storli, P.T., 2006. *Modelltest av Francis turbin i Vannkraftlaboratoriet ved NTNU, Trondheim*

White, F.M., 2008. *Fluid Mechanics.* 6th ed. New York: McGraw-Hill

World Bank, 2012. *Access to electricity (% of population).* [online].
Available at: <http://data.worldbank.org/indicator/EG.ELC.ACCS.ZS/countries>
[Accessed March 2012]

Appendices

Appendix A

Start up procedure

1. Turn on the frequency transformer in the basement (where the pumps are)

2. Make sure the right valves are open

   (a) Open the flow control valve

   (b) Make sure the valve in the pressure tank is open

3. Make sure the turbine is free to spin and that all the valves attached to the turbine system are closed

4. Start the generator (approximately 200rpm)

5. Start the pump (make sure it never goes under 100rpm!)

6. When the pressure tank is about 80% full, close the valve

7. Let the air out of the tubes connected to the pressure transducer

8. Fill in today's water temperature, atmospheric pressure and the tail water height in the LabView program

9. Do the desired measurements with varying rotational speed or pressure head (the pressure head is increased by increasing the rotational speed of the pump)

Appendix B

Calibration reports

B.1 Torque transducer
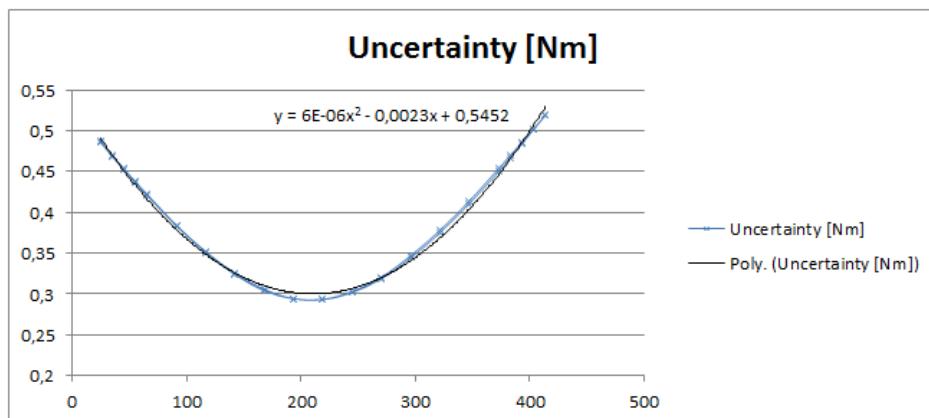
Figure B.1: Absolute uncertainty, torque

CALIBRATION REPORT

CALIBRATION PROPERTIES
Calibrated by: Cecilie Kvangarsnes
Type/Producer: T10F/FS
SN:
Range: 0-1000 Nm
Unit: Nm

CALIBRATION SOURCE PROPERTIES
Type/Producer: Deadweights
SN: -
Uncertainty [%]: 0

POLY FIT EQUATION:
Y= -2.08223707E+0X^0 -105.10908427E+0X^1

CALIBRATION SUMARY:
Max Uncertainty   : Inf [%]
Max Uncertainty   : 0.519175 [Nm]
RSQ   : 0.999952
Calibration points : 44
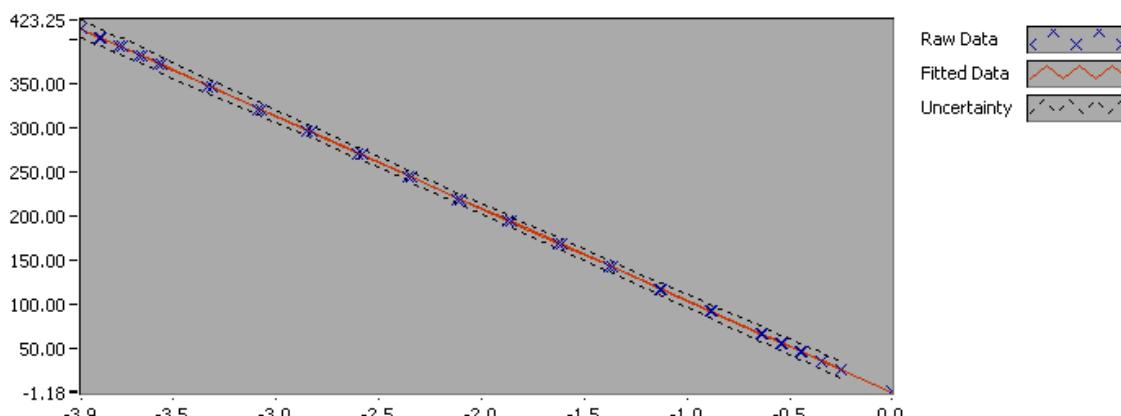
Figure 1 : Calibration chart (The uncertainty band is multiplied by 20)

_____
Cecilie Kvangarsnes

CALIBRATION VALUES

Value [Nm]	Voltage [V]	Best Poly Fit [Nm]	Deviation [Nm]	Uncertainty [%]	Uncertainty [Nm]
0.000000	-0.008568	-1.181640	1.181640	Inf	NaN
24.524909	-0.251430	24.345311	0.179597	1.984605	0.486723
34.764415	-0.348006	34.496308	0.268107	1.352727	0.470268
45.007066	-0.443767	44.561716	0.445350	1.007567	0.453476
55.249722	-0.539198	54.592387	0.657335	0.792057	0.437609
65.480767	-0.635589	64.723911	0.756856	0.644623	0.422104
91.091927	-0.881381	90.558873	0.533054	0.421957	0.384369
116.703446	-1.125807	116.250291	0.453155	0.301482	0.351840
142.314401	-1.364198	141.307406	1.006995	0.228655	0.325409
167.922283	-1.610168	167.161035	0.761248	0.181947	0.305530
193.534007	-1.855395	192.936600	0.597407	0.152011	0.294192
219.146704	-2.101978	218.854758	0.291945	0.133787	0.293190
244.761296	-2.340329	243.907603	0.853693	0.123279	0.301740
270.372712	-2.583429	269.459575	0.913137	0.117861	0.318664
295.984179	-2.828754	295.245523	0.738657	0.116266	0.344129
321.597440	-3.070647	320.670611	0.926828	0.116648	0.375135
347.208958	-3.313078	346.152376	1.056582	0.118306	0.410768
372.818940	-3.555925	371.677794	1.141146	0.120699	0.449990
383.061591	-3.656050	382.201839	0.859752	0.121920	0.467029
393.303249	-3.752095	392.297063	1.006185	0.123038	0.483911
403.546002	-3.851507	402.746124	0.799878	0.124327	0.501716
413.784386	-3.945236	412.597928	1.186459	0.125346	0.518663
413.784386	-3.947831	412.870705	0.913681	0.125470	0.519175
403.546002	-3.857712	403.398348	0.147654	0.124536	0.502559
393.303249	-3.763625	393.508912	-0.205663	0.123561	0.485968
383.061591	-3.671826	383.860034	-0.798443	0.122705	0.470037
372.818940	-3.578025	374.000670	-1.181730	0.121692	0.453692
347.208958	-3.334424	348.395987	-1.187029	0.119235	0.413995
321.597440	-3.093072	323.027772	-1.430333	0.117555	0.378054
295.984179	-2.853979	297.896855	-1.912676	0.117229	0.346980
270.372712	-2.606966	271.933584	-1.560872	0.118611	0.320692
244.761296	-2.362989	246.289413	-1.528117	0.123748	0.302887
219.146704	-2.120484	220.799865	-1.653161	0.133843	0.293313
193.534007	-1.878302	195.344392	-1.810385	0.151916	0.294009
167.922283	-1.631107	169.361952	-1.439669	0.181002	0.303942
142.314401	-1.382772	143.259632	-0.945231	0.227352	0.323554
116.703446	-1.136844	117.410370	-0.706924	0.300233	0.350382

Justervesenet

KALIBRERINGSBEVIS
Certificate of calibration
Nr./No: CAL 016-06/730-3

NORSK
AKKREDITERING
CAL 016
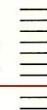
Kalibreringslaboratoriets navn: Name of the calibration laboratory: **JUSTERVESENET** Oslo justerkammer	Laboratoriets adresse: Laboratory address: Fetveien 99 2007 KJELLER	Side/Page: 1 av/of: 4 Ref. til måleprotokoll/Ref to records: 06/730

Tid og sted for kalibrering/*Date and place of calibration:*	Bevisets utstedelsesdato: *Date of issue:*
Kjeller, 9. – 15. august 2006	Kjeller, 28. august 2006
Kalibrering utført av/*Calibration performed by:*	Ansvarlig/*Responsible:*
Arne Georg Andersen, avdelingsingeniør	Nils M. Thomassen, justermester

Kunde: NTNU Vannkraftlaboratoriet, Alfred Getz v. 4, 7491 Trondheim.
Customer

Instrument: Lodd
Item

Kapasitet: 650 g – 5,7 kg
Capacity

Produsent: Ikke kjent
Manufacturer

Typebetegnelse: Se resultater side 2.
Model

Serienummer: Ikke kjent
Serial number

Intern nummer: Se side 2.
Internal number

Tidligere kalibreringsbevis nr.: CAL 016-32/05/1. NTNU VKL 103 er ikke kalibrert tidligere.
Previous calibration no.

KALIBRERINGSBEVIS
Certificate of Calibration

Justervesenet
Oslo justerkammer

Nr./No.: CAL 016-06/730-3

Side/Page: 2   av/of: 4

Måleresultater med usikkerhet:

Nominell verdi	Kjennetegn	Konvensjonell verdi			Usikkerhet (k = 2)	k-faktor ref EA 4/02	V_{eff}
5 kg	NTNU VKL 1	5 kg	+	0,32 g	± 0,15 g	k = 2	∞
5 kg	NTNU VKL 2	5 kg	+	0,42 g	± 0,15 g	k = 2	∞
5 kg	NTNU VKL 3	5 kg	+	0,24 g	± 0,15 g	k = 2	∞
5 kg	NTNU VKL 4	5 kg	−	0,22 g	± 0,15 g	k = 2	∞
5 kg	NTNU VKL 5	5 kg	+	0,63 g	± 0,15 g	k = 2	∞
5 kg	NTNU VKL 6	5 kg	+	0,61 g	± 0,15 g	k = 2	∞
5 kg	NTNU VKL 7	5 kg	+	0,96 g	± 0,15 g	k = 2	∞
5 kg	NTNU VKL 8	5 kg	+	0,42 g	± 0,15 g	k = 2	∞
5 kg	NTNU VKL 9	5 kg	+	0,93 g	± 0,15 g	k = 2	∞
5 kg	NTNU VKL 10	5 kg	+	0,72 g	± 0,15 g	k = 2	∞
5 kg	NTNU VKL 11	5 kg	+	0,39 g	± 0,15 g	k = 2	∞
5 kg	NTNU VKL 12	5 kg	+	0,10 g	± 0,15 g	k = 2	∞
5 kg	NTNU VKL 13	5 kg	+	0,07 g	± 0,15 g	k = 2	∞
5 kg	NTNU VKL 14	5 kg	+	0,15 g	± 0,15 g	k = 2	∞
5 kg	NTNU VKL 15	5 kg	+	0,20 g	± 0,15 g	k = 2	∞
5 kg	NTNU VKL 16	5 kg	+	0,29 g	± 0,15 g	k = 2	∞
2 kg	NTNU VKL 21	2 kg	−	0,858 g	± 0,070 g	k = 2	∞
2 kg	NTNU VKL 22	2 kg	−	0,246 g	± 0,068 g	k = 2	∞
2 kg	NTNU VKL 23	2 kg	−	0,241 g	± 0,060 g	k = 2	∞
2 kg	NTNU VKL 24	2 kg	−	2,487 g	± 0,062 g	k = 2	∞
5 kg	NTNU VKL 28	5 kg	−	2,03 g	± 0,15 g	k = 2	∞
5 kg	NTNU VKL 29	5 kg	−	1,38 g	± 0,15 g	k = 2	∞
5 kg	NTNU VKL 30	5 kg	−	0,98 g	± 0,15 g	k = 2	∞
5 kg	NTNU VKL 31	5 kg	−	0,36 g	± 0,15 g	k = 2	∞
5 kg	NTNU VKL 32	5 kg	−	1,63 g	± 0,15 g	k = 2	∞
5 kg	NTNU VKL 33	5 kg	−	1,13 g	± 0,15 g	k = 2	∞
5 kg	NTNU VKL 34	5 kg	−	0,84 g	± 0,15 g	k = 2	∞
5 kg	NTNU VKL 35	5 kg	−	1,61 g	± 0,15 g	k = 2	∞
5 kg	NTNU VKL 36	5 kg	−	1,71 g	± 0,15 g	k = 2	∞
5 kg	NTNU VKL 37	5 kg	−	1,52 g	± 0,15 g	k = 2	∞
5 kg	NTNU VKL 38	5 kg	−	1,76 g	± 0,15 g	k = 2	∞
5 kg	NTNU VKL 39	5 kg	−	1,83 g	± 0,15 g	k = 2	∞
5 kg	NTNU VKL 40	5 kg	−	1,91 g	± 0,15 g	k = 2	∞
5 kg	NTNU VKL 41	5 kg	−	1,57 g	± 0,15 g	k = 2	∞
5 kg	NTNU VKL 42	5 kg	−	1,56 g	± 0,15 g	k = 2	∞
5 kg	NTNU VKL 43	5 kg	−	1,74 g	± 0,15 g	k = 2	∞
5 kg	NTNU VKL 44	5 kg	−	0,76 g	± 0,15 g	k = 2	∞
5 kg	NTNU VKL 45	5 kg	−	1,84 g	± 0,15 g	k = 2	∞

KALIBRERINGSBEVIS
Certificate of Calibration

Nr./No.: CAL 016-06/730-3

Nominell verdi	Kjennetegn	Konvensjonell verdi	Usikkerhet (k = 2)	k-faktor ref EA 4/02	V_{eff}
5 kg	NTNU VKL 46	5 kg – 1,74 g	± 0,15 g	k = 2	∞
5 kg	NTNU VKL 47	5 kg – 0,99 g	± 0,15 g	k = 2	∞
5 kg	NTNU VKL 48	5 kg – 1,08 g	± 0,15 g	k = 2	∞
5 kg	NTNU VKL 49	5 kg – 1,33 g	± 0,15 g	k = 2	∞
5 kg	NTNU VKL 50	5 kg – 0,47 g	± 0,15 g	k = 2	∞
2 kg	NTNU VKL 51	2 kg – 0,908 g	± 0,065 g	k = 2	∞
2 kg	NTNU VKL 52	2 kg – 1,093 g	± 0,089 g	k = 2,28	10,38
2 kg	NTNU VKL 53	2 kg – 0,576 g	± 0,060 g	k = 2	∞
2 kg	NTNU VKL 54	2 kg – 0,258 g	± 0,060 g	k = 2	∞
2 kg	NTNU VKL 55	2 kg – 0,113 g	± 0,060 g	k = 2	∞
2 kg	NTNU VKL 56	2 kg – 0,776 g	± 0,059 g	k = 2	∞
2 kg	NTNU VKL 57	2 kg – 0,449 g	± 0,062 g	k = 2	∞
2 kg	NTNU VKL 58	2 kg – 0,248 g	± 0,059 g	k = 2	∞
2 kg	NTNU VKL 59	2 kg – 1,136 g	± 0,062 g	k = 2	
5,7 kg	NTNU VKL 101	5,7 kg + 74,96 g	± 0,15 g	k = 2	∞
650 g	NTNU VKL 103	650 g – 0,019 g	± 0,0039 g	k = 2,10	18

Loddene oppfyller ikke spesifikasjoner ihht OIML R111 og er derfor ikke vurdert ihht denne.

Målemetode:
Substitusjonsveiing, prosedyre JV-LM-MAS-004 utgave nr. 4.0

Sporbarhet:
Loddene er sammenlignet med loddnormaler som er sporbare til de nasjonale normaler for masse.

Forhold under kalibreringen:
Kalibreringen er basert på en antatt densitet 8000 kg/m^3 på loddene ved 20 °C og antatt densitet på 1,2 kg/m^3 på luften.

Temperatur under kalibreringen var fra 19,5 – 20,0 °C ± 0,1 °C
Fuktigheten under kalibreringen var fra 45,8 – 47,8 % RH ± 1,5 % RH

Måleusikkerhet, metode for beregning og hovedkomponenter:

Den rapporterte utvidede usikkerheten er fastslått som standard måleusikkerhet multiplisert med dekningsfaktor som angitt i tabellen over, som for en t-fordeling med effektive frihetsgrader (v_{eff}) som angitt i tabellen over, korresponderer til en dekningssannsynlighet på tilnærmet 95%. Standard måleusikkerhet har blitt bestemt i samsvar med EA publikasjonen "EA 4/02"

B.2 Pressure transducer
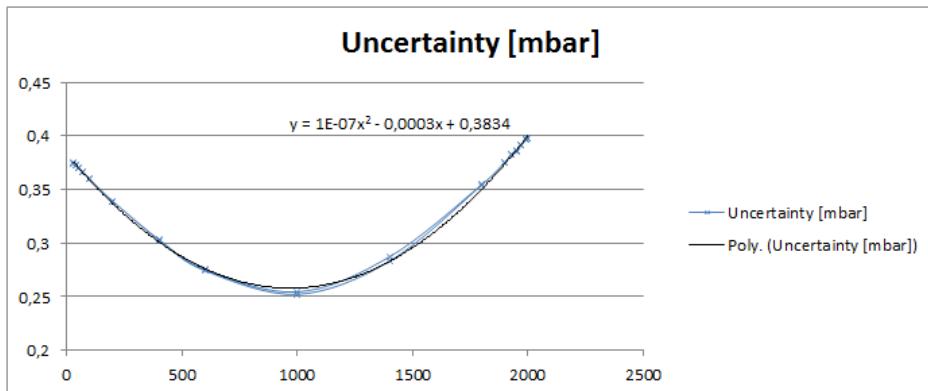
Figure B.2: Absolute uncertainty, inlet pressure

CALIBRATION REPORT

CALIBRATION PROPERTIES
Calibrated by: Cecilie Kvangarsnes
Type/Producer: Druck DPI 601
SN:
Range: 0-2 bar
Unit: mbar

CALIBRATION SOURCE PROPERTIES
Type/Producer:
SN: -
Uncertainty [%]:

POLY FIT EQUATION:
Y= -995.10178147E+0X^0 + 499.83841396E+0X^1

CALIBRATION SUMARY:
Max Uncertainty   : Inf [%]
Max Uncertainty   : 0.398236 [mbar]
RSQ   : 0.999999
Calibration points : 36
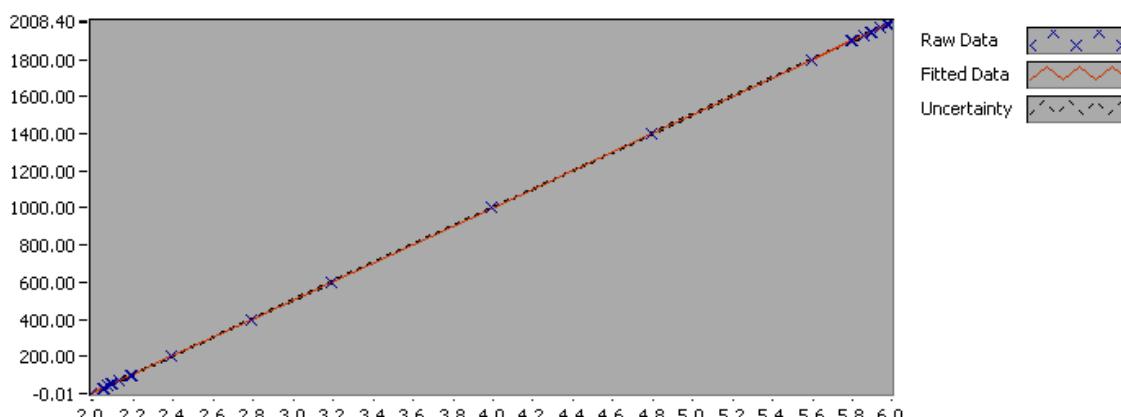
Figure 1 : Calibration chart (The uncertainty band is multiplied by 20)

_____
Cecilie Kvangarsnes

CALIBRATION VALUES

Value [mbar]	Voltage [V]	Best Poly Fit [mbar]	Deviation [mbar]	Uncertainty [%]	Uncertainty [mbar]
0.000000	1.990824	-0.011622	0.011622	Inf	NaN
30.000000	2.048740	28.937318	1.062682	1.249906	0.374972
40.000000	2.071357	40.242107	-0.242107	0.931234	0.372494
50.000000	2.089943	49.531889	0.468111	0.740930	0.370465
70.000000	2.129742	69.425026	0.574974	0.523091	0.366163
100.000000	2.189440	99.264438	0.735562	0.359812	0.359812
200.000000	2.389984	199.503844	0.496156	0.169610	0.339219
400.000000	2.789394	399.144362	0.855638	0.075840	0.303361
600.000000	3.188502	598.633757	1.366243	0.045872	0.275235
1000.000000	3.989807	999.157244	0.842756	0.025440	0.254404
1400.000000	4.789424	1398.836238	1.163762	0.020518	0.287252
1800.000000	5.592100	1800.044457	-0.044457	0.019708	0.354741
1900.000000	5.790787	1899.355880	0.644120	0.019776	0.375753
1930.000000	5.850569	1929.237474	0.762526	0.019822	0.382564
1950.000000	5.890670	1949.281382	0.718618	0.019758	0.385286
1970.000000	5.932180	1970.029694	-0.029694	0.019863	0.391310
1990.000000	5.971788	1989.827451	0.172549	0.019903	0.396077
2000.000000	5.993022	2000.440871	-0.440871	0.019901	0.398017
2000.000000	5.991754	1999.807027	0.192973	0.019912	0.398236
1990.000000	5.972769	1990.317382	-0.317382	0.019911	0.396225
1970.000000	5.934269	1971.073801	-1.073801	0.019862	0.391272
1950.000000	5.893452	1950.672109	-0.672109	0.019841	0.386905
1930.000000	5.854268	1931.086344	-1.086344	0.019810	0.382330
1900.000000	5.793678	1900.801046	-0.801046	0.019759	0.375426
1800.000000	5.592377	1800.182990	-0.182990	0.019688	0.354377
1400.000000	4.791135	1399.691299	0.308701	0.020230	0.283222
1000.000000	3.990758	999.632288	0.367712	0.025227	0.252274
600.000000	3.192204	600.484496	-0.484496	0.045690	0.274141
400.000000	2.790649	399.771953	0.228047	0.075671	0.302686
200.000000	2.391385	200.204340	-0.204340	0.169524	0.339048
100.000000	2.191207	100.147469	-0.147469	0.359565	0.359565
70.000000	2.133114	71.110591	-1.110591	0.522549	0.365784
50.000000	2.093499	51.309653	-1.309653	0.740139	0.370069
40.000000	2.071763	40.444724	-0.444724	0.931103	0.372441
30.000000	2.054644	31.888224	-1.888224	1.247728	0.374318
0.000000	1.991832	0.492453	-0.492453	Inf	NaN

Druck

CALIBRATION CERTIFICATE

(POSITIVE PRESSURE)

UNIT UNDER TEST (UUT)

Manufacturer	: Druck
Type Number	: DPI601
Serial Number	: 14206/96-1
Sales Order Number	: M11798-1
Parameter Range	: 0 to 10 bar g
Calibration Date	: 24 January 1996
Calibrated By	: S.Pattison
External Sensor Serial No.	:

CALIBRATOR INFORMATION

1.
Manufacturer	: Budenburg
Calibration Instrument	: Type 246
Serial Number	: 10442
Calibrated Against (*1)	: Druck Stds. Lab.
Pressure Medium	: Dry Nitrogen

AMBIENT CONDITIONS

Ambient Temperature (°C)	: 19.0
Local Gravity (ms^{-2})	: 9.81291

PERFORMANCE DATA

Nominal Applied Value bar	Actual Applied Value bar (*2)	Unit Under Test Reading bar (*3)	Unit Under Test Deviation (*4)	Permissible Deviation	Pass/ Fail
0.000	0.000	0.000	0.000 %fs	± 0.050%fs ± 1 digit	Pass
2.000	2.000	2.000	0.000 %fs	± 0.050%fs ± 1 digit	Pass
4.000	4.000	4.000	0.000 %fs	± 0.050%fs ± 1 digit	Pass
6.000	6.000	6.000	0.000 %fs	± 0.050%fs ± 1 digit	Pass
8.002	8.002	8.001	- 0.010 %fs	± 0.050%fs ± 1 digit	Pass
10.002	10.002	10.003	0.010 %fs	± 0.050%fs ± 1 digit	Pass

COMMENTS

I hereby certify that the details above are correct.

Certified by: S. PATTISON   Signed: S Patti   Date: 24 January 1996

NOTES

(*1) Traceable to relevant International Standards.
(*2) Actual Applied Value corrected for gravity and temperature as appropriate.
      Where applicable, other scales to BS350 calculated equivalent engineering units are used.
(*3) Actual recorded values. For specification, see Permissible Deviation column.
(*4) Deviation calculated from U.U.T. Reading minus Actual Applied Value.

CAL1 6/92

B.3   Trip meter
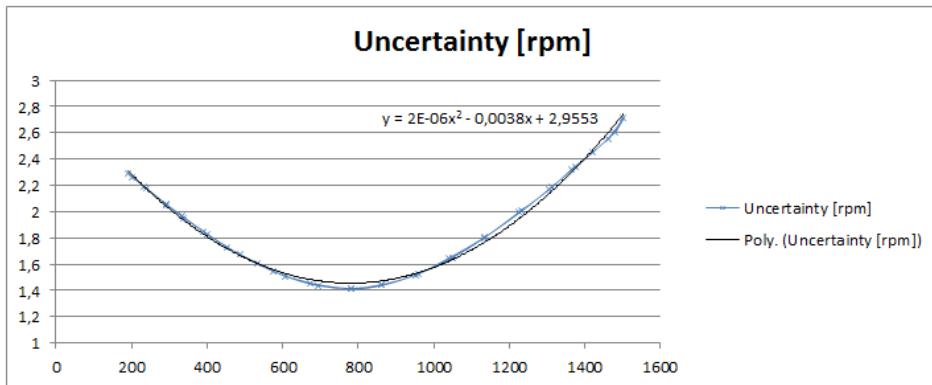
Figure B.3: Absolute uncertainty, rotational speed

CALIBRATION REPORT

CALIBRATION PROPERTIES
Calibrated by: Cecilie Kvangarsnes
Type/Producer:
SN:
Range: 0-1500rpm
Unit: rpm

CALIBRATION SOURCE PROPERTIES
Type/Producer:
SN: -
Uncertainty [%]: 0

POLY FIT EQUATION:
Y= + 4.18733037E+0X^0 + 1.00390144E+3X^1

CALIBRATION SUMARY:
Max Uncertainty   : Inf [%]
Max Uncertainty   : 2.717294 [rpm]
RSQ   : 0.999907
Calibration points : 39
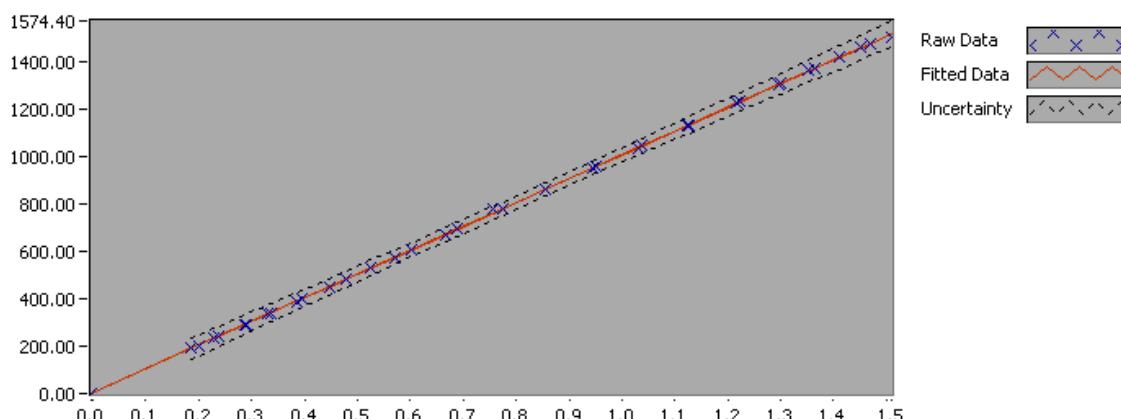
Figure 1 : Calibration chart (The uncertainty band is multiplied by 20)

_____
Cecilie Kvangarsnes

CALIBRATION VALUES

Value [rpm]	Voltage [V]	Best Poly Fit [rpm]	Deviation [rpm]	Uncertainty [%]	Uncertainty [rpm]
0.000000	-0.003032	1.143008	-1.143008	Inf	NaN
203.000000	0.200283	205.252014	-2.252014	1.114360	2.262150
241.000000	0.237432	242.545223	-1.545223	0.902470	2.174953
291.000000	0.286128	291.431165	-0.431165	0.707533	2.058921
335.000000	0.329814	335.288063	-0.288063	0.586926	1.966203
400.000000	0.394251	399.976525	0.023475	0.457700	1.830800
486.000000	0.478965	485.020594	0.979406	0.344598	1.674746
576.000000	0.569679	576.088684	-0.088684	0.268157	1.544586
673.000000	0.666028	672.813353	0.186647	0.216310	1.455769
782.000000	0.755478	762.613102	19.386898	0.180790	1.413780
863.000000	0.855594	863.119519	-0.119519	0.166912	1.440453
960.000000	0.951589	959.488670	0.511330	0.159111	1.527465
1049.000000	1.038831	1047.071473	1.928527	0.157176	1.648774
1135.000000	1.126054	1134.634453	0.365547	0.158977	1.804390
1233.000000	1.222902	1231.860342	1.139658	0.162670	2.005727
1311.000000	1.300569	1309.830132	1.169868	0.166752	2.186112
1374.000000	1.364311	1373.821394	0.178606	0.170261	2.339391
1461.000000	1.449835	1459.678632	1.321368	0.175028	2.557161
1502.000000	1.509971	1520.049510	-18.049510	0.180912	2.717294
1479.000000	1.468977	1478.895638	0.104362	0.176279	2.607168
1421.000000	1.409676	1419.362936	1.637064	0.172717	2.454303
1365.000000	1.353989	1363.458993	1.541007	0.170278	2.324293
1306.000000	1.295516	1304.757883	1.242117	0.166172	2.170211
1226.000000	1.216985	1225.920283	0.079717	0.162920	1.997397
1133.000000	1.123782	1132.353899	0.646101	0.159013	1.801614
1039.000000	1.030804	1039.013228	-0.013228	0.158348	1.645233
953.000000	0.945391	953.266851	-0.266851	0.159364	1.518742
863.000000	0.854616	862.137702	0.862298	0.167384	1.444528
781.000000	0.773491	780.695776	0.304224	0.181132	1.414639
695.000000	0.687903	694.774012	0.225988	0.206744	1.436872
607.000000	0.600649	607.179634	-0.179634	0.248616	1.509101
532.000000	0.525744	531.982668	0.017332	0.302481	1.609199
452.000000	0.446254	452.182126	-0.182126	0.382912	1.730764
390.000000	0.385696	391.388181	-1.388181	0.474048	1.848788
339.000000	0.335372	340.867518	-1.867518	0.576025	1.952724
292.000000	0.288953	294.267269	-2.267269	0.703276	2.053565
232.000000	0.228588	233.666781	-1.666781	0.945297	2.193088

B.4 Gravity

NTNU
Vannkraftlaboratoriet v/ Brandåstrø
Alfred Getzv. 4
7491 TRONDHEIM

Deres ref.:
Vår ref.:   04/00568-001 PLAR JSR/JG/blø
Arkiv: 296100

Trondheim, 26. august 2004

TYNGDENS AKSELERASJON I g I VANNKRAFTLABORATORIET VED NTNU, TRONDHEIM

Norges geologiske undersøkelse (NGU) målte 26.08.2004 g-verdien i ett punkt i 1. etg. i Vannkraftlaboratoriet ved NTNU i Alfred Getz v. 4. Målingene ble utført med Scintrex CG-3 Autograv nr. 9601306 ved tilknytning til Statens kartverks punkt for absoluttmålinger ved NGU, hvor g er bestemt tidligere med stor nøyaktighet.

Den målte verdien av g (IGSN71) i laboratoriet er:

        Punkt på gulvet, **982 146,516** milliGal

        Usikkerheten anslås til 0,010 milliGal

Faktura for oppdraget oversendes separat.

Med vennlig hilsen
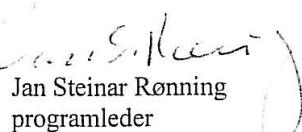
Jan Steinar Rønning
programleder
Planlegging og arealforvaltning
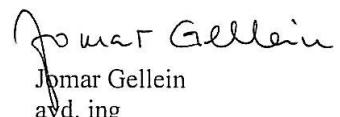
Jomar Gellein
avd. ing

B.5 Water temperature and atmospheric pressure

Certificate of Calibration

Certificate number: 3630

Unit under test:	Nokeval
Serial number:	Id.1
Procedure:	Manuel
Customer:	Process Partner
Cal Date	10.12.04
Cal Due Date	10.12.05

Calibration conditions:

Temperature: 23 +/- 2°C.   Humidity: 35±10%

Remarks:

NOR-TRONIX hereby certifies that the instrument described above has been calibrated using standards with traceable calibration to International Standards. This calibration certificate is issued with a measuring report, and shall only be fully reproduced.

Set Value	True Value		Read D.U.T.		Deviation
0	0,10	°C	0,2	°C	0,05
17	17,08	°C	17,1	°C	-0,02
20	19,95	°C	19,9	°C	-0,01
22,5	22,46	°C	22,42	°C	-0,04
25	24,94	°C	24,89	°C	-0,05
27	26,98	°C	26,95	°C	-0,03

Note: The deviation is calculated by subtracting the true value from the reading
D.U.T : Device Under Test

Standards used:

Instrument:	Model:	Cert no:	Traceability:
Resistance bridge	ASL F250 Mk2 Sn: 3290 014 1555	02/778-3	Justervesenet
Pt100 probe	Isotech Sn: 171115/4ASL	02/778-3	Justervesenet
Pt100 probe	ASL Y1592A/158	02/778-3	Justervesenet
Pt100 probe	Special		Nor-Tronix
Cryostatic temperature bath	Guissani BK40 Sn: B 737 S95	-	-

Måleusikkerhet : 0,1°C K=1

Performed by:

Heidi R Kristiansen

Certified by: *Ole Petter Walhus*

Kalibreringsbevis
Certificate of calibration

Teknologisk Institutt

Oppdragsgiver *Client*	Utførende enhet/lab. *Department/laboratory responsible*
NTNU Energi og Prosessteknikk Att.: Jørgen Ramdal Alfred Getz vei 4 NO-7491 TRONDHEIM	Teknologisk Institutt as Postboks 1019 3601 KONGSBERG

Bevisnr. *Certificate no.*	Kalibreringsdato *Date of calibration*	Utskriftsdato *Date of print*	Sidenr./antall sider *Page no./No. of pages*
06-018957	18.10.2006	18.10.2006	1 av *of* 1

Kalibrert utstyr *Calibrated equipment*

- **Tis objektID** *TI's obj. ID*   415024
- **Kundens ID** *Clients ID*   415024
- **Serienr.** *Serial no.*   Z3850004
- **Objekt** *Object*   Digital Barometer
- **Fabrikat** *Manufacturer*   Vaisala
- **Modell** *Model*   PTB220

Kalibrert av *Calibrated by*

Kalibreringsdata *Calibration data*

- **Kalibreringsprosedyre** *Calibration procedure*
- **Status** *Status*   Kalibrert uten justering
- **Temperatur og fuktighet** *Temperature and humidity*   23°C±3°, <70% RH
- **Anbefalt ny kalibrering** *Recommended new calibr.*   18.10.2007

Kalibreringsnormaler *Calibration standards*

ObjektID *Object ID*	Objekt *Object*	Fabrikat *Manufacturer*	Objekttype *Object type*	Neste kalib. *Next calibr.*
7810	BAROMETER			01.05.2007

Merknader *Comments*

max avvik : + 0,3 hPa ved 1000hPa nivå.
måleusikkerhet: +/- 0,1hPa

Instrumentet er kalibrert i henhold til dokumentert prosedyre som kan forevises på forespørsel, og mot målenormaler som er sporbare til nasjonale eller internasjonale normaler.

This instrument is calibrated according to documented procedure which will be available upon request, and against measuring normals traceable to national or international standard.

Appendix C

Calculation of uncertainties, Matlab and Excel

```
%------- CALCULATE MEAN DATA FROM RAW DATA (meandata_create.m) ---------------
-----%
%
%   Creates a new matrix 'meandata' from a source MxN:

%           1       .       .       .       N
%       ------- ------- ------- ------- -------
%     1 |   A   |   B   |   C   |   D   |   E   |
%     . ------- ------- ------- ------- -------
%       |  a_1  |  b_1  |  c_1  |   .   |   .   |
%     . |  a_2  |  b_2  |   .   |   .   |   .   |
%       |   .   |   .   |   .   |   .   |   .   |
%     . |   .   |   .   |   .   |   .   |   .   |
%       |   .   |   .   |   .   |   .   |   .   |
%     M |  a_M  |  b_M  |       |   .   |   .   |
%       ------- ------- ------- ------- -------

%   Where A-E indicates different settings, and (a,b,c,..)_m is
%   measurements at
%   different constant rotational speeds.
%
%   OUTPUT       meandata        Nx1 struct table
%                meandata_spl    Nx1 struct table
%                nan_map         (M-1)xN table of '0' and '1' where '1'
indicates
%                                that the source contains NaN values


%   source       rawdata matrix (from rawdata_import.m)

function [meandata meandata_spl nan_map] = meandata_create(source)


    %-------------------------------------------------------------

    D = 0.354;               %Diameter of turbine [m]
    Din = 0.4;               %Diameter in inlet [m]
    Dout = 0.596;            %Diameter in outlet [m]
    g = 9.82146514;          %Gravity in the NTNU laboratory
    z = 2.148;               %[m]
    t = 1.960;               %Degrees of freedom (random uncertainty)


    %-------------------------------------------------------------

    Ain = pi*(Din/2)^2;    %Areal in inlet [m^2]
    Aout = pi*(Dout/2)^2;  %Areal in outlet [m^2]
    bar = 10.19716213;     %[m]

    s = size(source);

    %Create 'meandata'

    for j = 1:s(2)
```

```matlab
        for i = 1:s(1)-1

                p = source{i+1,j}(:,2);            %bar
                q = source{i+1,j}(:,1)/1000;       %m^3/s
                M = source{i+1,j}(:,3);            %Nm
                n = source{i+1,j}(:,4);            %rpm

                %Mean values of raw data
                p_temp(i,1) = mean(p);
                q_temp(i,1) = mean(q);
                M_temp(i,1) = mean(M);
                n_temp(i,1) = mean(n);

                %Calculate error and standard deviation of raw data
                std_p = std(p);
                std_q = std(q);
                std_M = std(M);
                std_n = std(n);

                err_p = (t*std_p)/sqrt(length(p));
                err_q = (t*std_q)/sqrt(length(q));
                err_M = (t*std_M)/sqrt(length(M));
                err_n = (t*std_n)/sqrt(length(n));

                p_temp(i,2) = err_p;
                q_temp(i,2) = err_q;
                M_temp(i,2) = err_M;
                n_temp(i,2) = err_n;

                p_temp(i,3) = 100*err_p/p_temp(i,1);
                q_temp(i,3) = 100*err_q/q_temp(i,1);
                M_temp(i,3) = 100*err_M/M_temp(i,1);
                n_temp(i,3) = 100*err_n/n_temp(i,1);

        end

        %Insert calculated data into new table 'meandata'

        %From raw
        meandata{j,1}.p = p_temp;
        meandata{j,1}.q = q_temp;
        meandata{j,1}.torque = M_temp;
        meandata{j,1}.n = n_temp;
end
```

Setting 1

Calibration	Error	Uncertainty calibration [%]	Uncertainty test [%]	Total uncertainty [%]
Torque				
Dish [g]	4746,5	0,05		
Wire [g]	41,75	0,05		
Weights 5kg [g] *3	5000	0,15		
Weights 2 kg [g] *4	2000	0,065		
		0,0011		
Radius of shaft [mm]	52,5	0,1		
Additional arm [mm]	469	1		
		0,1927		
		0,1927		
Calibration [Nm]	148,1934	0,3356	0,2265		
			0,2974	0,0048	0,2974
Inlet pressure				
Calibrator			0,0001		
Calibration [mbar]	493,095	0,2598	0,0527		
			0,0527	0,1119	0,1237
Rotational speed				
Calibrator [rpm]	949,836	0,5	0,0526		
Calibration [rpm]	949,836	1,1503	0,1211		
			0,1321	0,0016	0,1321
Volume flow [m^3/s]	0,25624		0,0978	0,0035	0,0979
Water temp [degC]	20,58		0,0300		
Patm [kPa]	99,92		0,0500		

Calculation	Error	Uncertainty [%]
Outlet pressure [m]		
Tail water [m]	0,5100	0,0200	3,9216
Outlet radius [m]	0,2980	0,0001	0,0336
Inlet radius [m]	0,2000	0,0001	0,0500
Inlet velocity [m/s]	2,0391		0,1207
(Inlet velocity [m/s])^2		0,0100	
Outlet velocity [m/s]	0,9185		0,1088
(Outlet velocity [m/s])^2		0,0018	
	0,4671	0,0200	4,2822
Effective pressure head		
Inlet pressure [Pa]	49309,5000	60,9877	0,1237
Outlet pressure [Pa]	4580,2351	196,1351	4,2822
Inlet velocity [m/s]	2,0391	0,0025	0,1207
Outlet velocity [m/s]	0,9185	0,0010	0,1088
Height difference [m]	2,1480	0,0020	0,0931
	6,8797		0,3060
Efficiency		
Torque			0,2974
Rotational speed			0,1321
Density			0,0100
Volume flow			0,0979
Effective pressure head			0,3060
			0,4574

g	9,821465		r1 [m]	0,2
rho1	998,0782		r2 [m]	0,298
rho2	998,2261		A1 [m^2]	0,1257
1bar [m]	10,19716		A2 [m^2]	0,2790

Setting 2

Calibration		Error	Uncertainty calibration [%]	Uncertainty test [%]	Total uncertainty [%]
Torque					
Dish [g]	4746,5	0,05			
Wire [g]	41,75	0,05			
Weights 5kg [g] *5	5000	0,15			
Weights 2 kg [g] *4	2000	0,065	0,0010		
Radius of shaft [mm]	52,5	0,1			
Additional arm [mm]	469	1	0,1927		
			0,1927		
Calibration [Nm]	183,1634	0,3252	0,1775		
			0,2620	0,0037	0,2621
Inlet pressure					
Calibrator			0,0001		
Calibration [mbar]	336,948	0,2937	0,0872		
			0,0872	0,1286	0,1554
Rotational speed					
Calibrator [rpm]	799,093	0,5	0,0626		
Calibration [rpm]	799,093	1,1958	0,1496		
			0,1622	0,0016	0,1622
Volume flow [m^3/s]	0,31114		0,0978	0,0024	0,0978
Water temp [degC]	20,15		0,0300		
Patm [kPa]	100,99		0,0500		

Calculation		Error	Uncertainty [%]
Outlet pressure [m]			
Tail water [m]	0,5100	0,0200	3,9216
Outlet radius [m]	0,2980	0,0001	0,0336
Inlet radius [m]	0,2000	0,0001	0,0500
Inlet velocity [m/s]	2,4760		0,1207
(Inlet velocity [m/s])^2		0,0148	
Outlet velocity [m/s]	1,1153		0,1087
(Outlet velocity [m/s])^2		0,0027	
	0,4467		**4,4776**
Effective pressure head			
Inlet pressure [Pa]	33694,8000	52,3471	0,1554
Outlet pressure [Pa]	4380,4348	196,1376	4,4776
Inlet velocity [m/s]	2,4760	0,0030	0,1207
Outlet velocity [m/s]	1,1153	0,0012	0,1087
Height difference [m]	2,1480	0,0020	0,0931
	5,3872		**0,3864**
Efficiency			
Torque			0,2621
Rotational speed			0,1622
Density			0,01
Volume flow			0,0978
Effective pressure head			0,3864
			0,5039

Appendix D

Additional results

Figure D.1 shown the efficiency and volume flow at 800 rpm, at setting 1 and 2.
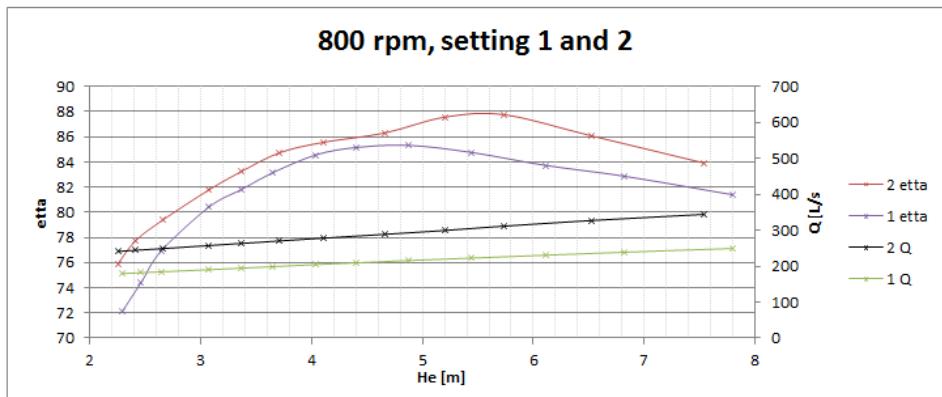

Figure D.1: Efficiency at 800 rpm at setting 1 and 2

Setting 2 has a higher volume flow, and higher efficiency.

Appendix E

Generator information

SIEMENS Motor i Småturbinriggen, 1PH71842HF010AA3

Hei Bård
Det er ok, motor kan henge etter labber med aksel opp eller ned !
Jeg sender litt spec. på motor så du har det i arkivet.

1PH71842HF010AA3

COMPACT INDUCTION MOTOR 51 KW, 1500 RPM, 324.7 NM, VC: 60 KW, 1750 RPM, 327.4 NM, 122 A, W/O BRAKE; 3AC 400 V, 50 HZ, WITH FAN REL. MOTOR ENCODER HTL 1024 - INCR/REV TERMINAL BOX ON TOP, CABLE ON THE RIGHT, **DESIGN IM B3 FOR VERTICAL MOUNTING (IM V5, IM V6),** BEARING F. COUPLING OUTPUT, VIBRATION SEVERITY GRADE R, SHAFT A. FLANGE ACCURACY GR. N FITTED KEY + HALF-KEY BALANCING AIR FLOW FROM DRIVE END TO NON- DRIVE END IP 55, FAN IP 54, STANDARD FINISH (RAL 7016)
Motor vekt 370 kg

mvh Ole Johan

email: ole.hungnes@siemens.com
Postal address: Siemens AS, N-7493 Trondheim, Norway
phone: +47 7395 9577, telefax: +47 7395 9511
mobile: +47 93045633

Appendix F

Risk assessment

Risikovurderingsrapport

Kaplanrigg

Prosjekttittel	Test av Kaplanturbin
Prosjektleder	Torbjørn Nielsen
Enhet	NTNU
HMS-koordinator	Bård Brandåstrø
Linjeleder	Olav Bolland
Riggnavn	Kaplanrigg
Plassering	Vannkraftlab
Romnummer	42
Riggansvarlig	Cecilie Kvangarsnes
Risikovurdering utført av	Cecilie Kvangarsnes

INNHOLDSFORTEGNELSE

1   INNLEDNING

Riggen står i hovedrommet til vannkraftlaboratoriet. Formålet med riggen er å gjøre virkningsgradmåling av turbinen.

2   ORGANISERING

Rolle	NTNU	Sintef
Lab Ansvarlig:	Morten Grønli	Harald Mæhlum
Linjeleder:	Olav Bolland	Mona J. Mølnvik
HMS ansvarlig:	Olav Bolland	Mona J. Mølnvik
HMS koordinator	Erik Langørgen	Harald Mæhlum
HMS koordinator	Bård Brandåstrø	
Romansvarlig:	Bård Brandåstrø	
Prosjekt leder:	Torbjørn Nielsen	
Ansvarlig riggoperatører:	Cecilie Kvangarsnes	

3   RISIKOSTYRING AV PROSJEKTET

Hovedaktiviteter risikostyring	Nødvendige tiltak, dokumentasjon	DTG
Prosjekt initiering	Prosjekt initiering mal	X
Veiledningsmøte	Skjema for Veiledningsmøte med pre-risikovurdering	X
Innledende risikovurdering	Fareidentifikasjon – HAZID Skjema grovanalyse	X
Vurdering av teknisk sikkerhet	Prosess-HAZOP Tekniske dokumentasjoner	X
Vurdering av operasjonell sikkerhet	Prosedyre-HAZOP Opplæringsplan for operatører	
Sluttvurdering, kvalitetssikring	Uavhengig kontroll Utstedelse av apparaturkort Utstedelse av forsøk pågår kort	

4   TEGNINGER, FOTO, BESKRIVELSER AV FORSØKSOPPSETT

Vedlegg:
Prosess og Instrumenterings Diagram, (PID)
Komponentliste med spesifikasjoner
Tegninger og bilder som beskriver forsøksoppsetningen.

5   EVAKUERING FRA FORSØKSOPPSETNINGEN

Se kapittel 14 "Veiledning til rapport mal.
Evakuering skjer på signal fra alarmklokker eller lokale gassalarmstasjon med egen lokal varsling med lyd og lys utenfor aktuelle rom, se 6.2
Evakuering fra rigg området foregår igjennom merkede nødutganger.

6 VARSLING

6.1 Før forsøkskjøring

Varsling per e-post, med opplysning om forsøkskjøringens varighet og involverte til:
- HMS koordinator NTNU/SINTEF
  HaraldStein.S.Mahlum@sintef.no
  Erik.langorgen@ntnu.no
  Baard.brandaastro@ntnu.no
- *Prosjektledere på naborigger varsles for avklaring rundt bruk av avtrekksanlegget uten fare eller forstyrrelser av noen art, se rigg matrise.*

All forsøkskjøringen skal planlegges og legges inn i aktivitetskalender for lab. Forsøksleder må få bekreftelse på at forsøkene er klarert med øvrig labdrift før forsøk kan iverksettes.

6.2 Ved uønskede hendelser

BRANN
Ved brann en ikke selv er i stand til å slukke med rimelige lokalt tilgjengelige slukkemidler, skal nærmeste brannalarm utløses og arealet evakueres raskest mulig. En skal så være tilgjengelig for brannvesen/bygningsvaktmester for å påvise brannsted.
Om mulig varsles så:

NTNU	SINTEF
Labsjef Morten Grønli, tlf: 918 97 515	
HMS: Erik Langørgen, tlf: 91897160	
Instituttleder: Olav Bolland: 91897209	

GASSALARM
Ved gassalarm skal gassflasker stenges umiddelbart og området ventileres. Klarer man ikke innen rimelig tid å få ned nivået på gasskonsentrasjonen så utløses brannalarm og laben evakueres. Dedikert personell og eller brannvesen sjekker så lekkasjested for å fastslå om det er mulig å tette lekkasje og lufte ut området på en forsvarlig måte.
Varslingsrekkefølge som i overstående punkt.

PERSONSKADE
- Førstehjelpsutstyr i Brann/førstehjelpsstasjoner,
- Rop på hjelp,
- Start livreddende førstehjelp
- **Ring 113** hvis det er eller det er tvil om det er alvorlig skade.

ANDRE UØNSKEDE HENDELSER (AVVIK)
NTNU:
Rapporteringsskjema for uønskede hendelser på
http://www.ntnu.no/hms/2007_Nettsider/HMSRV0401_avvik.doc

SINTEF:
Synergi

7 VURDERING AV TEKNISK SIKKERHET

7.1 Fareidentifikasjon, HAZOP

Se kapittel 14 "Veiledning til rapport mal.

Forsøksoppsetningen deles inn i følgende noder:

Node 1	Rørsystem med pumpe
Node 2	Roterende turbin
Node 3	Generatoroppsett

Vedlegg, skjema: Hazop_mal

Node1:

Rørelementer er eksternt levert og godkjent for aktuelt trykk.

Node2:

Roterende deler er for det meste ikke tilgjengelig. Roterende deler i friluft er lett synlig, og utenfor normal arbeidssone.

Node3:

Generatoroppsett er forsvarlig montert, vanskelig tilgjengelig fra gulv.

7.2 Brannfarlig, reaksjonsfarlig og trykksatt stoff og gass

Se kapittel 14 "Veiledning til rapport mal.

Inneholder forsøkene brannfarlig, reaksjonsfarlig og trykksatt stoff

Ja	Trykksatt vann

Vedlegg Ex-sonekart:

Vurdering: *Arbeidsmedium er vann. Alle rør er levert av eksternt firma med prøvesertifikat.*

7.3 Trykkpåkjent utstyr

Inneholder forsøksoppsetningen trykkpåkjent utstyr:

Ja	**Utstyret trykktestes i henhold til norm og dokumenteres**

Trykkutsatt utstyr skal trykktestes med driftstrykk gange faktor 1.4,for utstyr som har usertifiserte sveiser er faktoren 1.8. Trykktesten skal dokumenteres skriftlig hvor fremgangsmåte framgår*.*

Vedlegg: Prøvesertifikat for trykktesting finnes i labperm.

Vurdering:

7.4 Påvirkning av ytre miljø (utslipp til luft/vann, støy, temperatur, rystelser, lukt)

Se kapittel 14 "Veiledning til rapport mal..

NEI	

Vurdering: Det blir ingen utslipp til ytre miljø.

7.5 Stråling

Se kapittel 14 "Veiledning til rapport mal.

NEI	

Vedlegg:

Vurdering: Ingen strålekilder.

7.6 Bruk og behandling av kjemikalier

Se kapittel 14 "Veiledning til rapport mal.

Nei	

Vedlegg:
Vurdering:

7.7 El sikkerhet (behov for å avvike fra gjeldende forskrifter og normer)

NEI	

Her forstås montasje og bruk i forhold til normer og forskrifter med tanke på berøringsfare
Vedlegg:
Vurdering: Alt elektrisk utstyr er forsvarlig montert og står slik permanent.

8   VURDERING AV OPERASJONELL SIKKERHET

Sikrer at etablerte prosedyrer dekker alle identifiserte risikoforhold som må håndteres gjennom operasjonelle barrierer og at operatører og teknisk utførende har tilstrekkelig kompetanse.

8.1 Prosedyre HAZOP

Se kapittel 14 "Veiledning til rapport mal.
Metoden er en undersøkelse av operasjonsprosedyrer, og identifiserer årsaker og farekilder for operasjonelle problemer.
Vedlegg: HAZOP_MAL_Prosedyre
Vurdering: Operatør har et eget rom for å kjøre riggen.

8.2 Drifts og nødstopps prosedyre

Se kapittel 14 "Veiledning til rapport mal.
Nødstopp koordineres med labpersonell, for å unngå at man må ta en omvei via laben for nødstopp ved evakuering.
Vedlegg "Procedure for running experiments"

8.3 Opplæring av operatører

Dokument som viser Opplæringsplan for operatører utarbeides for alle forøksoppsetninger*.
- *Kjøring av pumpesystem.*

Vedlegg*: Opplæringsplan for operatører

8.4 Tekniske modifikasjoner

Vurdering: Modifikasjoner gjøres i samråd med Torbjørn Nielsen/Bård Brandåstrø

8.5 Personlig verneutstyr

Vurdering: *Det er påbudt med vernebriller i sonen anlegget er plassert i.*

8.6 Generelt

Vurdering: Alle forsøk kjøres med operatør til stede.

8.7 Sikkerhetsutrustning

- *Vernebriller*

8.8 Spesielle tiltak

9 TALLFESTING AV RESTRISIKO – RISIKOMATRISE

Se kapittel 14 "Veiledning til rapportmal.
Risikomatrisen vil gi en visualisering og en samlet oversikt over aktivitetens risikoforhold slik at ledelse og brukere får et mest mulig komplett bilde av risikoforhold.

IDnr	Aktivitet-hendelse	Frekv-Sans	Kons	RV
1	*Roterende aksling*	2	B	B2
2	*Fremmedlegemer i vannet*	1	A	A1
3	*Rørbrudd*	1	A	A1

Vurdering restrisiko: *Deltakerne foretar en helhetsvurdering for å avgjøre om gjenværende risiko ved aktiviteten/prosessen er akseptabel. Fremmedlegemer i vannet gir liten risiko for personskade, men kan føre til store skader på maskineri.*

10 KONKLUSJON

Riggen er bygget til god laboratorium praksis (GLP).

Hvilke tekniske endringer eller endringer av driftsparametere vil kreve ny risikovurdering: Ingen

Apparaturkortet får en gyldighet på **4 måneder**
Forsøk pågår kort får en gyldighet på **4 måneder**

11 LOVER FORSKRIFTER OG PÅLEGG SOM GJELDER

Se http://www.arbeidstilsynet.no/regelverk/index.html
- Lov om tilsyn med elektriske anlegg og elektrisk utstyr (1929)
- Arbeidsmiljøloven
- Forskrift om systematisk helse-, miljø- og sikkerhetsarbeid (HMS Internkontrollforskrift)
- Forskrift om sikkerhet ved arbeid og drift av elektriske anlegg (FSE 2006)
- Forskrift om elektriske forsyningsanlegg (FEF 2006)

- Forskrift om utstyr og sikkerhetssystem til bruk i eksplosjonsfarlig område NEK 420
- Forskrift om håndtering av brannfarlig, reaksjonsfarlig og trykksatt stoff samt utstyr og anlegg som benyttes ved håndteringen
- Forskrift om Håndtering av eksplosjonsfarlig stoff
- Forskrift om bruk av arbeidsutstyr.
- Forskrift om Arbeidsplasser og arbeidslokaler
- Forskrift om Bruk av personlig verneutstyr på arbeidsplassen
- Forskrift om Helse og sikkerhet i eksplosjonsfarlige atmosfærer
- Forskrift om Høytrykksspyling
- Forskrift om Maskiner
- Forskrift om Sikkerhetsskilting og signalgivning på arbeidsplassen
- Forskrift om Stillaser, stiger og arbeid på tak m.m.
- Forskrift om Sveising, termisk skjæring, termisk sprøyting, kullbuemeisling, lodding og sliping (varmt arbeid)
- Forskrift om Tekniske innretninger
- Forskrift om Tungt og ensformig arbeid
- Forskrift om Vern mot eksponering for kjemikalier på arbeidsplassen (Kjemikalieforskriften)
- Forskrift om Vern mot kunstig optisk stråling på arbeidsplassen
- Forskrift om Vern mot mekaniske vibrasjoner
- Forskrift om Vern mot støy på arbeidsplassen

Veiledninger fra arbeidstilsynet
se: http://www.arbeidstilsynet.no/regelverk/veiledninger.html

12 VEDLEGG

13 DOKUMENTASJON

- Tegninger, foto, beskrivelser av forsøksoppsetningen
- Hazop_mal
- Sertifikat for trykkpåkjent utstyr
- Håndtering avfall i NTNU
- Sikker bruk av LASERE, retningslinje
- HAZOP_MAL_Prosedyre
- Forsøksprosedyre
- Opplæringsplan for operatører
- Skjema for sikker jobb analyse, (SJA)
- Apparaturkortet
- Forsøk pågår kort

14 VEILEDNING TIL RAPPORTMAL

Kap 5 Evakuering fra forsøksoppsetningen
Beskriv i hvilken tilstand riggen skal forlates ved en evakueringssituasjon.

Kap 7 Vurdering av teknisk sikkerhet

Sikre at design av apparatur er optimalisert i forhold til teknisk sikkerhet.

Identifisere risikoforhold knyttet til valgt design, og eventuelt å initiere re-design for å sikre at størst mulig andel av risiko elimineres gjennom teknisk sikkerhet.

Punktene skal beskrive hva forsøksoppsetningen faktisk er i stand til å tåle og aksept for utslipp.

7.1 Fareidentifikasjon, HAZOP

Forsøksoppsetningen deles inn i noder: (eks M*otorenhet, pumpeenhet, turbinenhet.*)

Ved hjelp av ledeord identifiseres årsak, konsekvens og sikkerhetstiltak. Konkluderes det med at tiltak er nødvendig anbefales disse på bakgrunn av dette. Tiltakene lukkes når de er utført og Hazop sluttføres.

(eks "No flow", årsak: rør er deformert, konsekvens: pumpe går varm, sikkerhetsforanstaltning: måling av flow med kobling opp mot nødstopp eller hvis konsekvensen ikke er kritisk benyttes manuell overvåkning og punktet legges inn i den operasjonelle prosedyren.)

7.2 Brannfarlig, reaksjonsfarlig og trykksatt stoff.

I henhold til Forskrift om håndtering av brannfarlig, reaksjonsfarlig og trykksatt stoff samt utstyr og anlegg som benyttes ved håndteringen

Brannfarlig stoff: Fast, flytende eller gassformig stoff, stoffblanding, samt stoff som forekommer i kombinasjoner av slike tilstander, som i kraft av sitt flammepunkt, kontakt med andre stoffer, trykk, temperatur eller andre kjemiske egenskaper representerer en fare for brann.
Reaksjonsfarlig stoff: Fast, flytende, eller gassformig stoff, stoffblanding, samt stoff som forekommer i kombinasjoner av slike tilstander, som ved kontakt med vann, ved sitt trykk, temperatur eller andre kjemiske forhold, representerer en fare for farlig reaksjon, eksplosjon eller utslipp av farlig gass, damp, støv eller tåke.
Trykksatt stoff: Annet fast, flytende eller gassformig stoff eller stoffblanding enn brann- eller reaksjonsfarlig stoff, som er under trykk, og som derved kan representere en fare ved ukontrollert utslipp.

Nærmere kriterier for klassifisering av brannfarlig, reaksjonsfarlig og trykksatt stoff er fastsatt i vedlegg 1 i veiledningen til forskriften "Brannfarlig, reaksjonsfarlig og trykksatt stoff"

http://www.dsb.no/Global/Publikasjoner/2009/Veiledning/Generell%20veiledning.pdf

http://www.dsb.no/Global/Publikasjoner/2010/Tema/Temaveiledning_bruk_av_farlig_stoff_Del_1.pdf

Rigg og areal skal gjennomgås med hensyn på vurdering av Ex sone

- Sone 0: Alltid eksplosiv atmosfære, for eksempel inne i tanker med gass, brennbar væske.
- Sone 1: Primær sone, tidvis eksplosiv atmosfære for eksempel et fylle tappe punkt
- Sone 2: Sekundert utslippssted, kan få eksplosiv atmosfære ved uhell, for eksempel ved flenser, ventiler og koblingspunkt

7.4 Påvirkning av ytre miljø

Med forurensning forstås: tilførsel av fast stoff, væske eller gass til luft, vann eller i grunnen støy og rystelser påvirkning av temperaturen som er eller kan være til skade eller ulempe for miljøet.

Regelverk: http://www.lovdata.no/all/hl-19810313-006.html#6

NTNU retningslinjer for avfall se: http://www.ntnu.no/hms/retningslinjer/HMSR18B.pdf

7.5 Stråling

Stråling defineres som

Ioniserende stråling: Elektromagnetisk stråling (i strålevernsammenheng med bølgelengde <100 nm) eller hurtige atomære partikler (f.eks alfa- og beta-partikler) som har evne til å ionisere atomer eller molekyler
Ikke-ioniserende stråling: Elektromagnetisk stråling (bølgelengde >100 nm), og ultralyd1, som har liten eller ingen evne til å ionisere.
Strålekilder: Alle ioniserende og sterke ikke-ioniserende strålekilder.
Ioniserende strålekilder: Kilder som avgir ioniserende stråling, f.eks alle typer radioaktive kilder, røntgenapparater, elektronmikroskop
Sterke ikke-ioniserende strålekilder: Kilder som avgir sterk ikke-ioniserende stråling som kan skade helse og/eller ytre miljø, f.eks laser klasse 3B og 4, MR2-systemer, UVC3-kilder, kraftige IR-kilder4
1 Ultralyd er akustisk stråling ("lyd") over det hørbare frekvensområdet (>20 kHz). I strålevernforskriften er ultralyd omtalt sammen med elektromagnetisk ikke-ioniserende stråling.
2 MR (eg. NMR) - kjernemagnetisk resonans, metode som nyttes til å «avbilde» indre strukturer i ulike materialer.
3 UVC er elektromagnetisk stråling i bølgelengdeområdet 100-280 nm.
4 IR er elektromagnetisk stråling i bølgelengdeområdet 700 nm – 1 mm.

For hver laser skal det finnes en informasjonsperm(HMSRV3404B) som skal inneholde:
- Generell informasjon
- Navn på instrumentansvarlig og stedfortreder, og lokal strålevernskoordinator
- Sentrale data om apparaturen
- Instrumentspesifikk dokumentasjon
- Referanser til (evt kopier av) datablader, strålevernbestemmelser, o.l.
- Vurderinger av risikomomenter
- Instruks for brukere
- Instruks for praktisk bruk; oppstart, drift, avstenging, sikkerhetsforholdsregler, loggføring, avlåsing, evt. bruk av strålingsmåler, osv.
- Nødprosedyrer

Se ellers retningslinjen til NTNU for laser: http://www.ntnu.no/hms/retningslinjer/HMSR34B.pdf

7.6 Bruk og behandling av kjemikalier.

Her forstås kjemikalier som grunnstoff som kan utgjøre en fare for arbeidstakers sikkerhet og helse.

Se ellers: http://www.lovdata.no/cgi-wift/ldles?doc=/sf/sf/sf-20010430-0443.html

Sikkerhetsdatablar skal være i forøkenes HMS perm og kjemikaliene registrert i Stoffkartoteket.

Kap 8 Vurdering av operasjonell sikkerhet

Sikrer at etablerte prosedyrer dekker alle identifiserte risikoforhold som må håndteres gjennom operasjonelle barrierer og at operatører og teknisk utførende har tilstrekkelig kompetanse.

8.1 Prosedyre Hazop

Prosedyre-HAZOP gjennomføres som en systematisk gjennomgang av den aktuelle prosedyren ved hjelp av fastlagt HAZOP-metodikk og definerte ledeord. Prosedyren brytes ned i enkeltstående arbeidsoperasjoner (noder) og analyseres ved hjelp av ledeordene for å avdekke mulige avvik, uklarheter eller kilder til mangelfull gjennomføring og feil.

8.2 Drifts og nødstopp prosedyrer

Utarbeides for alle forsøksoppsetninger.

Driftsprosedyren skal stegvis beskrive gjennomføringen av et forsøk, inndelt i oppstart, under drift og avslutning. Prosedyren skal beskrive forutsetninger og tilstand for start, driftsparametere med hvor store avvik som tillates før forsøket avbrytes og hvilken tilstand riggen skal forlates.

Nødstopp-prosedyre beskriver hvordan en nødstopp skal skje, (utført av uinnvidde),
hva som skjer, (strøm/gass tilførsel) og
hvilke hendelser som skal aktivere nødstopp, (brannalarm, lekkasje).

Kap 9 Risikomatrise

9 Tallfesting av restrisiko, Risikomatrisen

For å synliggjøre samlet risiko, jevnfør skjema for risikovurdering, plottes hver enkelt aktivitets verdi for sannsynlighet og konsekvens inn i risikomatrisen. Bruk aktivitetens IDnr.
Eksempel: Hvis aktivitet med IDnr. 1 har fått en risikoverdi D3 (sannsynlighet 3 x konsekvens D) settes aktivitetens IDnr i risikomatrisens felt for 3D. Slik settes alle aktivitetenes risikoverdier (IDnr) inn i risikomatrisen.

I risikomatrisen er ulike grader av risiko merket med rød, gul eller grønn. Når en aktivitets risiko havner på rød (= uakseptabel risiko), skal risikoreduserende tiltak gjennomføres. Ny vurdering gjennomføres etter at tiltak er iverksatt for å se om risikoverdien er kommet ned på akseptabelt nivå.

KONSEKVENS	Svært alvorlig	E1	E2	E3	E4	E5
	Alvorlig	D1	D2	D3	D4	D5
	Moderat	C1	C2	C3	C4	C5
	Liten	B1	B2	B3	B4	B5
	Svært liten	A1	A2	A3	A4	A5
		Svært liten	Liten	Middels	Stor	Svært Stor
		SANSYNLIGHET				

Prinsipp over akseptkriterium. Forklaring av fargene som er brukt i risikomatrisen.

Farge		Beskrivelse
Rød		Uakseptabel risiko. Tiltak skal gjennomføres for å redusere risikoen.
Gul		Vurderingsområde. Tiltak skal vurderes.
Grønn		Akseptabel risiko. Tiltak kan vurderes ut fra andre hensyn.